

1 Dear editor,

2 We wish to thank you, the two anonymous referees, and Dr H. Moosmüller for useful comments on the
3 manuscript. We have carefully revised the text to improve the clarity of the reading.

4 In particular we have made a small change to the paper title from

5 “Spectral- and size-resolved mass absorption efficiency of mineral dust aerosols in the shortwave: a
6 simulation chamber study”

7 to

8 “Spectral- and size-resolved mass absorption efficiency of mineral dust aerosols in the shortwave **spec-**
9 **trum**: a simulation chamber study”

10

11 The detailed answers to the two anonymous referees are presented

12

13 Anonymous Referee #1

14 The paper presents needed results on dust optical properties (mass absorption efficiency and absorp-
15 tion Angstrom exponent) for $D < 2.5 \mu\text{m}$ and $D < 10 \mu\text{m}$ particles, relating them to chemical composition.
16 The samples analyzed are from 12 locations in northern Africa (5 samples), Namibia (1 sample), north-
17 ern China (1 sample), the Middle East (2 samples), North America (1 sample), South America (1 sam-
18 ple) and Australia (1 sample). I have no substantial issues with the analysis or the paper. I recommend
19 publication after addressing the minor points below:

20

21 1) In the Abstract and somewhere earlier in the paper (before the Results section) the location where
22 the samples were collected from should be presented. Some information about sample collection is
23 also needed – i.e.: a) Was only one sample collected at each location, or were multiple samples col-
24 lected then combined? b) Were the samples collected from locations know to be preferential sources
25 for atmospheric dust or was the collection location just random? The latter point is important, since it’s
26 know that atmospheric dust comes from preferential locations.

27 **To address this point, the sentence in the result section has been rewritten as “The selection of these**
28 **soils and sediments was made out of 137 individual top-soil samples collected in major arid and semi-**
29 **arid regions worldwide and representing the mineralogical diversity of the soil composition at the global**
30 **scale. As discussed in Di Biagio et al. (2017), this large sample set was reduced by a set of 19 samples**

31 their availability in sufficient quantities for injection in the chamber. Because some of the experiments
32 did not produce enough dust to perform good-quality optical measurements, , in this paper we present
33 a set of twelve samples distributed worldwide but mostly in Northern and Western Africa (Libya, Algeria,
34 Mali, Bodélé) and the Middle East (Saudi Arabia and Kuwait). Individual samples from the Gobi desert
35 in Eastern Asia, the Namib Desert, the Strzelecki desert in Australia, the Patagonian deserts in South
36 America, and the Sonoran Desert in Arizona have also been investigated.”

37 The first sentence of the abstract has been changed as ”This paper presents new laboratory measure-
38 ments of the mass absorption efficiency (MAE) between 375 and 850 nm for twelve individual samples
39 of mineral dust from different source areas worldwide and in two size classes”.

40

41 2) Abstract, pg. 2, lines 33-34: “The size-independence of AAE suggests that, for a given size distribu-
42 tion, the possible variation of dust composition with size would not affect significantly the spectral be-
43 havior of shortwave absorption.” Either that or the composition simply DIDN’T vary with size for this set
44 of samples – so I’d reword this a bit.

45 This correction has been accepted

46

47 3) pg. 2, line 39: Need to spell out AAOD this first time that you use it.

48 This correction has been accepted

49

50 4) pg. 2, lines 40-41: “which is relevant to the development of remote sensing of light-absorption aero-
51 sols from space. ” Not only from space! This approach has also been used extensively for AERONET
52 (surface-based remote sensing) AAOD attribution.

53 The reviewer is right, the sentence has been rewritten as “, which is relevant to the development of
54 remote sensing of light-absorption aerosols from space, and their assimilation in climate models.”

55

56 5) pg. 3 line 56 contains a partial sentence (“In the solar spectrum (Boucher et al., 2013)”).

57 This was reworded as “Albeit partially compensated by the radiative effect in the thermal infrared, the
58 global mean radiative effect of mineral dust in the shortwave is negative both at the surface and the top
59 of the atmosphere (TOA) and local warming of the atmosphere (Boucher et al., 2013).”

60

61 6) pg. 6, lines 162-163: “The total uncertainty, including the effects of photon counting and the deposit
62 inhomogeneity, on the absorption coefficient measurement is estimated at 8%.” Is there a basis/refer-
63 ence for this?

64 The references to the papers of Petzold et al. (2004) and Massabo’ et al. (2013) have been added to
65 the text.

66

67 7) pg. 7, line 170: It would be useful to give typical total masses and/or the fractional error/uncertainty
68 in total aerosol gravimetric mass based on this error in filter mass.

69 This has been added in lines 173-175.

70

71 8) pg. 8, line 223 equation: When I read this my immediate question was: “How does this compare to
72 the measure of total gravimetric mass?”. You answer this question (appropriately) in the results section
73 but I still think it would be useful to add a note here pointing to the fact the in your results discussion
74 you found this agreed well with the total gravimetric mass.

75 The following sentence has been added “As it will be explained in the result section (paragraph 3.1),
76 the values of MCdust estimated from Equation 4 were found in excellent agreement with the measured
77 gravimetric mass on the filters”

78

79 9) pg. 10: Do you have any estimate / sense of how well the dust suspended by this “shaking” compares
80 to the dust lofted by winds?

81 Prior to any scientific analysis, we have dedicated a lot of energy to investigate the realism of our dust
82 generation system, both in terms of the composition and the size distribution of the dust aerosols. These
83 results are reported in two papers:

- 84
- 85 • Di Biagio, C., P. Formenti, S. A. Styler, E. Panguì, and J.-F. Doussin (2014), Laboratory chamber
86 measurements of the longwave extinction spectra and complex refractive indices of African and
87 Asian mineral dusts, *Geophys. Res. Lett.*, 41, doi:10.1002/2014GL060213. – Figure 2 and dis-
88 cussion

88 But in particular in

- 89 • Di Biagio, C., Formenti, P., Balkanski, Y., Caponi, L., Cazaunau, M., Pangu, E., Journet, E.,
90 Nowak, S., Caquineau, S., Andreae, M. O., Kandler, K., Saeed, T., Piketh, S., Seibert, D., Wil-
91 liams, E., and Doussin, J.-F.: Global scale variability of the mineral dust long-wave refractive
92 index: a new dataset of in situ measurements for climate modeling and remote sensing, *Atmos.*
93 *Chem. Phys.*, 17, 1901-1929, doi:10.5194/acp-17-1901-2017, 2017

94 where we have dedicated two paragraphs (5.1. Atmospheric representativity: mineralogical composition
95 and 5.2 Atmospheric representativity: size distribution) to show how the composition and the size dis-
96 tribution of the generated dust are well representative of those of real dust in the atmosphere, which
97 makes the laboratory experiments well suited for studying the dust optical properties.

98 In order to stress this point further, without repeating results already presented in these two publications,
99 we have added the following sentence in paragraph 3 “Di Biagio et al. (2014; 2017) have demonstrated
100 the realism of the generation system concerning the composition and the size distribution of the gener-
101 ated dust with respect to the properties of mineral dust in the atmosphere”.

102

103 10) pg. 11, line 209: Mauritania is not listed as one of the sample site locations in Table 3. ?

104 For Mauritania, we only have chemical composition but not optical measurement results. The reference
105 to this sample has been taken out of the paper.

106

107 11) pg. 11, lines 309-310 (an onward): The results here are said to agree well with that found for at-
108 mospheric aerosols in other studies, but the values in these studies is not given so this feels very hand-
109 waving and unconvincing. Are you referring to the values given in Table 5? If so, please refer directly
110 to them. If not, the comparison here needs to be more quantitative (discuss numbers from the literature
111 vs. what is found here).

112 Additional text and values have been added in lines 321-392 to address this point

113

114 12) pg. 13, lines 353-354: If you have results for Niger why not show them?

115 We do not have optical results for Niger

116

117 13) pg. 14, lines 387-388: MAE doesn't vary linearly inversely with wavelength, it varies linearly in-
118 versely with the log of the wavelength (hence our ability to use the AAE relationship).

119 The reviewer is correct, this has been corrected as “and decrease in a linear way with the logarithm of
120 the wavelength”

121

122 14) pg. 15, lines 429-434: A few things: a) “satisfactory” and “loose” are not quantitative terms, nor are
123 they really appropriate for a scientific paper. What constitutes “satisfactory”? Best is to just give the
124 correlations. b) The high correlation coefficients for PM_{2.5} are really driven by one high data point and
125 so are probably not very robust.

126 These sentences have been reworded as “Regardless of the size fraction, the correlation between the
127 MAE values and the percent mass of total elemental iron are higher at 375, 407 and 532 nm” and “At
128 these wavelengths, linear correlations with the mass fraction of iron oxides are low in the PM_{10.6} mass
129 fraction (R^2 up to 0.38-0.62), but higher in the PM_{2.5} fraction (R^2 up to 0.83-0.99)”

130

131 15) pg. 16, lines 455-456: How can fine-mode-only AAOD be GREATER than total aerosol AAOD?

132 Total and fine were inverted by mistake, this is now corrected

133

134 16) pg. 17, lines 487-488: As written this implies Solomon et al. varied SSA by 5%.

135 For, say, SSA of 0.9, that they varied SSA by 0.045. That is, the co-albedo (or absorption) was varied
136 by 45% (0.1 ± 0.045). This is the proper comparison to make to the variation in MAE that you calculate

137 The reviewer is right. The sentence has been corrected as “As a comparison, Solmon et al. (2008)
138 showed that varying the single scattering albedo of mineral dust over western Africa by $\pm 5\%$, that is,
139 varying the co-albedo (or absorption) by 45% (0.1 ± 0.045) could drastically change the climate re-
140 sponse in the region.”

141

142 7) Overall: Some editing is needed for language throughout. Here I list some that stood out to me – all
143 small stuff but editing would help readability:

144 pg. 3, line 67-68: “in the last ten years or so” (too casual for scientific writing)

145 removed

146

147 pg. 3, line 74: “A significant body of observations have been performed.”

148 Replaced by “A significant number of observations have quantified”

149

150 pg. 8, lines 214-215: “The linear deconvolution, performed the Athena IFEFFIT free-ware analysis pro-
151 gram (Ravel and Newville, 2005), provided with the proportionality factors α_i representing the
152 mass fraction of elemental iron to be assigned to the i-th standard mineral.” (I found this sentence nearly
153 impossible to follow)

154 Replaced by “The linear deconvolution has been performed with the Athena IFEFFIT freeware analysis
155 program (Ravel and Newville, 2005). This provided with the proportionality factors α_i representing the
156 mass fraction of elemental iron to be assigned to the i-th standard mineral.”

157

158 pg. 10, line 253: “the chamber was evacuated by to” (delete “by”)

159 Corrected

160

161 pg. 10, line 259: “dust particles produced was” → “dust particles produced were”

162 The sentence was corrected as “The dust particles produced by the mechanical shaking, mimicking the
163 saltation processing that soils experience when eroded by strong winds, were injected in the chamber
164 by flushing the flask with N₂ at 10 L min⁻¹ for about 10-15 min, whilst continuing shaking the soil.”

165

166 pg. 10, lines 279 “dust on filter for” → “dust on the filter for”

167 Corrected as “dust on the filter membranes for subsequent chemical analysis”

168

169 pg. 10, line 280: “by placing the loaded filter holders”: This reads as if you are placing LOADED FIL-
170 TERS (vs holders with blank filters in them, which is what I assume you mean). Rerword.

171 Corrected as “by placing the filter holders loaded with filter membranes”

172

173 pg. 11, line 206: “the origin of used dust samples”. I think this should be “the origin of our dust samples”,
174 yes?

175 Corrected as “the origin of dust samples”

176

177 pg. 12, line 315: "Henceforth, and contrary to the soil samples"

178 pg. 12, lines 317-318: "could reflect more that of the parent sedimentary soil than not the other samples."

179 These two sentences were rewritten as "This powder is likely to be injected in the chamber with little or
180 no size fractionation. Henceforth, the aerosol generated from it should have a closer composition to the
181 original powder than the other samples.

182

183 pg. 12, line 335: "An the exception"

184 Corrected as "Exceptions are"

185

186 pg. 13, lines 353-354: "As a matter of fact, the number fraction of particles in the size classes above
187 0.5 μm in diameter are different in the dust aerosol generated in the Alfaro et al. (2004) study with
188 respect to ours."

189 Corrected as "As a matter of fact, the number fraction of particles in the size classes above 0.5 μm in
190 diameter is different in the dust aerosol generated in the Alfaro et al. (2004) study with respect to ours."

191

192 pg. 13, line 364: "On the contrary" \rightarrow "In contrast

193 Corrected

194

195 pg. 13, line 365: "These differences could yield either to difference in the"

196 Corrected as "These differences could either be due to difference in the chemical composition and/or
197 in the total mass in the denominator of Equation 8."

198

199 pg. 15, lines 415-417: "using a power-law function fit as from Equation 2, provides withthe values of"

200 Corrected as "using the power-law function fit (Equation 2)"

201

202 pg. 16, line 448: "The size-dependence, yielding significantly higher MAE values"

203 Corrected as “The size-dependence, yielding significantly higher MAE values in the fine fraction
204 (PM_{2.5}) than in the bulk (PM_{10.6}) aerosol,”

205

206 pg. 17, line 470: “A closer look to observations” → “A closer look at observations”

207 Corrected as “These differences could either be due to difference in the chemical composition and/or
208 in the total mass in the denominator of Equation 8.”

209

210 pg. 17, line 478: “our estimated MAE average at” → “our average MAE values are”

211 Corrected

212

213 pg. 17, line 490: “As Moosmuller et al.” → “As in Moosmuller et al.”

214 Corrected

215

216 pg. 18, line 503-504: “pointing out to the” → “pointing out the

217 Corrected

218

219 Anonymous Referee #2

220 GENERAL COMMENT

221 The manuscript presents important results from a carefully designed and conducted study on the light-
222 absorbing properties of mineral dust from various origins. Dust samples collected at the different source
223 regions have been re-suspended in an aerosol chamber and characterized with respect to microphysi-
224 cal, optical and chemical properties by state of the art methods. The study provides urgently needed
225 knowledge on the multi-spectral light absorbing properties of mineral dust and for sure deserves publi-
226 cation in ACP. The manuscript is well structured, the methods are described in necessary detail and
227 the referenced literature reflects the current state of knowledge. I recommend publication after the fol-
228 lowing minor revisions have been considered.

229

230 SPECIFIC REMARKS

231 1. In the experimental protocol section, the potential impact of gravitational settling on the re-suspended
232 fraction of the dust samples is mentioned.

233 Given the instrumentation list, the size distributions of the airborne dust samples were monitored during
234 the runs of the experiments. It appears obvious to control the change of the size distribution during the
235 experiment time in the chamber. Since the mass concentration in the chamber decreased very rapidly
236 after injection, whereas the chemical composition of the dust samples was determined from bulk sam-
237 ples, it would be important to know if the airborne fraction sampled for the determination of optical
238 properties features the same chemical properties as the bulk samples. At least a discussion of this
239 potential source of uncertainties should be presented, along with a plot showing the change of the size
240 distributions during the experiment time. The current analysis starts from the assumption that the dust
241 bulk properties represent also the properties of the sampled airborne fractions. However, is this really
242 justified?

243 The reviewer is right when saying that the samples collected for the investigation of the chemical com-
244 position are time-integrated and henceforth might reproduce dust with varying size distributions. Exam-
245 ples of the time variability of the size distributions are provided by Di Biagio et al. (2017) - Figures 7 and
246 5S in the supplementary material. These figures show that, after the very strong initial depletion of
247 particles larger than 10 μm in diameter (when no sampling on filters was performed), the number con-
248 centration decreases at a rate, which is almost independent of size, suggesting that no significant dis-
249 tortion of the particle size distribution occurs after the most significant removal at the beginning of the
250 experiment.

251 We also would like to stress that our generation system allows to generate a dust aerosol from a soil,
252 and that this dust aerosol is injected in the chamber, not the soil. Henceforth, when talking about "bulk"
253 we refer to the total aerosol fraction, sampled from the chamber without any size segregation other than
254 that imposed by the cutoff the sampling lines. The fine fraction corresponds to the same dust aerosols,
255 but sampled by an impactor with a 2.5 diameter cutoff.

256

257 2. In section 3.2, the variability of dust optical properties with particle size is discussed. The authors
258 found no statistically significant size-dependence of the absorption Ångström exponent (AAE), whereas
259 the absolute values of the mass absorption efficiencies (MAE) show large differences between the PM2.5
260 and PM10 fractions with larger values for the fine mode fraction.

261 These findings imply that the relative chemical composition with respect to light-absorbing compounds
262 does not change between the size fractions (similar AAE values), whereas the differences between the
263 MAC values indicate that coarse mode particles contain more non-absorbing matter than fine mode
264 particles (higher MAE values for smaller particles). This however, this is in contrast to the assumption
265 that the chemical composition is uniformly distributed across the particle size distribution. Here, a de-
266 tailed discussion is requested.

267 The reviewer's statement is in error as for a given mineral composition (given effective complex refrac-
268 tive index) the MAE depends strongly on size, decreasing with size at larger sizes. So having a smaller
269 MAE for PM10 than for PM2.5, does not necessarily imply that PM10 contains less absorbing matter
270 than PM2.5, but may just be due to the change in size distribution. This is shown by our calculations.
271 An independent example of the size dependence is also given by Fig. 1 of Moosmuller et al. (2009).

272 Moosmüller, H., R. K. Chakrabarty, and W. P. Arnott (2009), Aerosol light absorption and its measure-
273 ment: A review, *Journal of Quantitative Spectroscopy and Radiative Transfer*, 110(11), 844-878.

274

275 3. In section 4, it is discussed that the potential impact of light absorption by mineral dust may play an
276 important role even after long range transport. Cited studies all refer to observations in China.

277 However, there is another detailed study on this effect available for the pollution plume of Dakar mixing
278 with mineral dust which also includes the variation of the AAE during mixing
279 (Petzold et al., 2011). The authors may consider including this study.

280 This reference has been added to the manuscript.

281

282 MINOR COMMENTS

283 1. The list of references contains various references which are not cited in the manuscript. This should
284 be checked, I found the following but there may be more: Anderson et al., 1998, Andrews et al., 2006,
285 Arnott et al., 2005, Collaud Coen et al., 2010, Petzold et al., 2013.

286 **Corrected**

287

288 2. Line 56: The sentence seems to be incomplete.

289 **The sentence was corrected as “Albeit partially compensated by the radiative effect in the thermal in-**
290 **frared, the global mean radiative effect of mineral dust in the shortwave is negative both at the surface**
291 **and the top of the atmosphere (TOA) and local warming of the atmosphere (Boucher et al., 2013).”**

292

293 3. Line 97 – 98: The basic unit of mass concentrations is gm⁻³. Using this unit, then the unit of the
294 combined property MAE is m² g⁻¹ as stated. In its current version this link is not clearly visible.

295 4. Line 102: The sentence seems to be incomplete.

296 **The sentence was removed**

297

298 5. Line 163: A reference for the uncertainty of the MWAA is required.

299 **This has been added**

300

301 6. Line 912: Please check for correct reference, there is no reference Petzold et al. (2008) in the list of
302 references.

303 **Corrected**

304

305 7. In Figure 4, regression lines may be shown as full line to improve their visibility.

306 **Done**

307

308 TYPOS

309 1. Line 108: It should read: “absorption Ångström exponent”.

310 Corrected

311

312 2. Line 138: Skip “with”.

313 Corrected

314

315 3. Line 165: It should read “deposited on a filter ...”.

316 Corrected

317

318 4. Line 245: It should read: “the uncertainty of values ...”.

319 Corrected

320

321 5. Line 253: Skip “by”.

322 Corrected

323

324 6. Line 338: It should read: “PM2.5 fraction”.

325 Corrected

326

327 7. Line 426 –427: I assume the Figures 4 are referenced here.

328 Corrected

329

330 REFERENCES

331 Petzold, A., Veira, A., Mund, S., Esselborn, M., Kiemle, C., Weinzierl, B., Hamburger, T., Ehret, G.,
332 Lieke, K., and Kandler, K.: Mixing of mineral dust with urban pollution aerosol over Dakar (Senegal):
333 impact on dust physico-chemical and radiative properties, *Tellus*, 63B, 619-634, doi: 10.1111/j.1600-
334 0889.2011.00547.x, 2011.

335 **Spectral- and size-resolved mass absorption efficiency of mineral dust aerosols in**
336 **the shortwave spectrum: a simulation chamber study**

337 Lorenzo Caponi^{1,2}, Paola Formenti¹, Dario Massabó², Claudia Di Biagio¹, Mathieu Cazaunau¹, Edou-
338 ard Pangui¹, Servanne Chevaillier¹, Gautier Landrot³, Meinrat O. Andreae^{4,11}, Konrad Kandler⁵, Stuart
339 Piketh⁶, Thuraya Saeed⁷, Dave Seibert⁸, Earle Williams⁹, Yves Balkanski¹⁰, Paolo Prati², and Jean-
340 François Doussin¹

341 ¹ *Laboratoire Interuniversitaire des Systèmes Atmosphériques (LISA), UMR 7583, CNRS, Université Paris-Est-*
342 *Créteil et Université Paris Diderot, Institut Pierre Simon Laplace, Créteil, France*

343 ² *University of Genoa, Department of Physics & INFN, Genoa, Italy*

344 ³ *Synchrotron SOLEIL, L'Orme des Merisiers Saint-Aubin, France*

345 ⁴ *Biogeochemistry Department, Max Planck Institute for Chemistry, P.O. Box 3060, 55020, Mainz, Germany*

346 ⁵ *Institut für Angewandte Geowissenschaften, Technische Universität Darmstadt, Schnittspahnstr. 9, 64287*
347 *Darmstadt, Germany*

348 ⁶ *Climatology Research Group, University of the Witwatersrand, Johannesburg, South Africa*

349 ⁷ *Science Department, College of Basic Education, Public Authority for Applied Education and Training, Al-*
350 *Ardeya, Kuwait*

351 ⁸ *Walden University, Minneapolis, Minnesota, USA*

352 ⁹ *Massachusetts Institute of Technology, Cambridge, Massachusetts, USA*

353 ¹⁰ *LSCE, CNRS UMR 8212, CEA, Université de Versailles Saint-Quentin, Gif sur Yvette, France*

354 ¹¹ *Geology and Geophysics Department, King Saud University, Riyadh, Saudi Arabia*

355
356 * Corresponding author: paola.formenti@lisa.u-pec.fr
357

358 Abstract

359 This paper presents new laboratory measurements of the mass absorption efficiency (MAE) between
360 375 and 850 nm for [twelve individual samples of](#) mineral dust [from different source areas worldwide](#)
361 [and in of different origin](#) in two size classes: PM_{10.6} (mass fraction of particles of aerodynamic diameter
362 lower than 10.6 μm) and PM_{2.5} (mass fraction of particles of aerodynamic diameter lower than 2.5 μm).
363 ~~The~~ experiments ~~have been~~ were performed in the CESAM simulation chamber using ~~generated~~-min-
364 eral dust generated from natural parent soils, and included optical and gravimetric analyses.

365 ~~The~~ Results show that the MAE values are lower for the PM_{10.6} mass fraction (range 37-135 10⁻³ m² g⁻¹
366 at 375 nm) than for the PM_{2.5} (range 95-711 10⁻³ m² g⁻¹ at 375 nm), and decrease with increasing wave-
367 length as λ^{-AAE} , where the Angstrom Absorption Exponent (AAE) averages between 3.3-3.5, regardless
368 of size. The size-independence of AAE suggests that, for a given size distribution, the ~~possible variation~~
369 ~~of dust composition~~ did not vary with size for this set of samples ~~with size would not affect significantly~~
370 ~~the spectral behavior of shortwave absorption~~. Because of its high atmospheric concentration, light-
371 absorption by mineral dust can be competitive ~~to~~ with black and brown carbon even during atmospheric
372 transport over heavy polluted regions, when dust concentrations are significantly lower than at emission.
373 The AAE values of mineral dust are higher than for black carbon (~1), but in the same range as light-
374 absorbing organic (brown) carbon. As a result, depending on the environment, there can be some ambi-
375 guity in apportioning the [aerosol absorption optical depth \(AAOD\)](#) based on spectral dependence, which
376 is relevant to the development of remote sensing of light-absor~~bing~~ption aerosols ~~from space~~, and their
377 assimilation in climate models. We suggest that the sample-to-sample variability in our dataset of MAE
378 values is related to regional differences ~~of~~ in the mineralogical composition of the parent soils. Particu-
379 larly in the PM_{2.5} fraction, we found a strong linear correlation between the dust light-absorption prop-
380 erties and elemental iron rather than the iron oxide fraction, which could ease the application and the
381 validation of climate models that now start to include the representation of the dust composition, as well
382 as for remote sensing of dust absorption in the UV-VIS spectral region.

383 1. Introduction

384 Mineral dust aerosols emitted by wind erosion of arid and semi-arid soils account for about 40% of the
385 total emitted aerosol mass per year at the global scale (Knippertz and Stuut, 2014). The episodic but
386 frequent transport of intense mineral dust plumes is visible from spaceborne sensors, as their high con-
387 centrations, combined with ~~to~~ their ability ~~of~~ to scatter~~ing~~ and absor~~bing~~ solar and thermal radiation,

388 give raise to the highest registered values of aerosol optical depth (AOD) on Earth (Chiapello, 2014).
389 The instantaneous radiative efficiency of dust particles, that is, their radiative effect per unit AOD, is of
390 the order of tenths to hundreds of $\text{W m}^{-2} \text{AOD}^{-1}$ in the solar spectrum, and of the order of order-of tenths
391 of $\text{W m}^{-2} \text{AOD}^{-1}$ in the thermal infrared (e.g., Haywood et al., 2003; di Sarra et al., 2011; Slingo et al.,
392 2006 and the compilation of Highwood and Ryder, 2014). ~~In the solar spectrum, (Boucher et al., 2013).~~
393 Albeit partially compensated by the radiative effect in the thermal infrared, the global mean radiative
394 effect of mineral dust in the shortwave is negative both at the surface and the top of the atmosphere
395 (TOA) and produces a local warming of the atmosphere (Boucher et al., 2013). ~~Many-There are the~~
396 ~~consequences- numerous impacts of dust on the~~ global and regional climate, ~~that-which~~ ultimately feed
397 back on wind speed and vegetation and therefore on dust emission (Tegen and Lacis, 1996; Solmon et
398 al., 2008; Pérez et al., 2006; Miller et al., 2014). Dust particles perturb the surface air temperature
399 through their radiative effect at TOA, can increase the atmospheric stability (e.g., Zhao et al. 2011) and
400 might affect precipitation at the global and regional scale (Solmon et al., 2008; Xian, 2008; Vinoj et al.,
401 2014; Miller et al., 2014 and references therein).

402 All models ~~show-indicate~~ that the effect of mineral dust on climate has a great sensitivity to their
403 shortwave absorption properties ~~of mineral dust~~ (Miller et al., 2004; Lau et al., 2009; Loeb and Su, 2010;
404 Ming et al., 2010; Perlwitz and Miller, 2010). Absorption by mineral dust started receiving a great deal
405 of interest ~~in the last ten years or so~~, when spaceborne and ground-based remote sensing studies (Dubo-
406 vik et al., 2002; Colarco et al., 2002; Sinyuk et al., 2003) suggested that mineral dust was less absorbing
407 ~~that-thani~~ had been ~~suggested indicated~~ by in situ observations (e.g., Patterson et al., 1977; Haywood et
408 al., 2001), particularly at wavelengths below 600 nm. Balkanski et al. (2007) showed that lowering the
409 dust absorption properties to an extent that reconciles them both with the remote-sensing observations
410 and the state-of-knowledge of the mineralogical composition, allowed calculating the clear-sky dust
411 shortwave radiative effect of dust in agreement with satellite-based observations. A significant body
412 number of observations has ~~ve-been-performed-in-quantify-quantifieding~~ the shortwave light-absorbing
413 properties of mineral dust, by direct measurements (Alfaro et al., 2004; Linke et al., 2006; Osborne et
414 al., 2008; McConnell et al., 2008; Derimian et al., 2008; Yang et al., 2009; Müller et al., 2009; Petzold
415 et al., 2009; Formenti et al., 2011; Moosmüller et al., 2012; Wagner et al., 2012; Ryder al., 2013a; Utry
416 et al., 2015; Denjean et al., 2015c; 2016), and indirectly, by quantifying the amount and the speciation
417 of the light-absorbing compounds in mineral dust, principally iron oxides (Lafon et al., 2004; 2006;

418 Lazaro et al., 2008; Derimian et al., 2008; Zhang et al., 2008; Kandler et al., 2007; 2009; 2011; Formenti
419 et al., 2014a; 2014b).

420 However, existing data are often limited to a single wavelength, which moreover ~~are-is~~ not the same
421 identical for all experiments. Also, frequently they do not represent the possible regional variability of
422 the dust absorption, either because they are obtained from field measurements integrating the contribu-
423 tions of different source regions, or conversely, by laboratory investigations targeting samples from a
424 limited number of locations. This might lead to biases in the data. Indeed, iron oxides in mineral dust,
425 mostly in the form of hematite (Fe₂O₃) and goethite (Fe(O)OH), have specific absorption bands in the
426 UV-VIS spectrum (Bédidi and Cervelle, 1993), and have a variable content depending on the soil min-
427 eralogy of the source regions (Journet et al., 2014).

428 ~~Henceforth, in this study, experiments on twelve aerosol samples generated from natural parent top~~
429 ~~soils from various source regions worldwide have been~~ ~~were~~ conducted with a large atmospheric simu-
430 lation chamber. ~~we~~ We present a new evaluation of the ultraviolet to near-infrared (375-850 nm) light-
431 absorbing properties of mineral dust by studying-investigating the size-segregated mass absorption effi-
432 ciency (MAE, units of m² g⁻¹) and its spectral dependence, largely-widely used in climate models to
433 calculate the direct radiative effect of aerosols. ~~Experiments on twelve aerosol samples generated from~~
434 ~~natural parent top soils from various source regions worldwide have been conducted with a large atmos-~~
435 ~~pheric simulation chamber.~~

436 2. Instruments and methods

437 At a given wavelength, λ , the mass absorption efficiency (MAE, units of m² g⁻¹) is defined as the ratio
438 of the aerosol light-absorption coefficient $b_{\text{abs}}(\lambda)$ (units of m⁻¹), and its mass concentration (in $\mu\text{g m}^{-3}$)

439

$$440 \quad MAE(\lambda) = \frac{b_{\text{abs}}(\lambda)}{\text{Mass Conc}} \quad (1)$$

441

442 ~~MAE values for mineral dust aerosol are expressed in~~ MAE values for mineral dust aerosol are ex-
443 pressed in 10⁻³ m² g⁻¹.

444 The spectral dependence of the aerosol absorption coefficient $b_{\text{abs}}(\lambda)$ is described by the power-law
445 relationship

446

447

$$b_{abs}(\lambda) \sim \lambda^{-AAE} \quad (2)$$

448

449 where the AAE is the [Absorption Ångström Absorption](#)-Exponent, representing the negative slope of
450 $b_{abs}(\lambda)$ in a log-log plot (Moosmüller et al., 2009)

451

$$AAE = -\frac{d\ln(b_{abs}(\lambda))}{d\ln(\lambda)} \quad (3)$$

453

454 **2.1. The CESAM simulation chamber**

455 [The e](#)Experiments in this work have been performed in the 4.2 m³ stainless-steel CESAM (French acro-
456 nym for Experimental Multiphasic Atmospheric Simulation Chamber) simulation chamber (Wang et al.,
457 2011). The CESAM chamber has been extensively used in recent years to simulate, at sub and super-
458 saturated conditions, the formation and properties of aerosols at concentration levels comparable to those
459 encountered in the atmosphere (Denjean et al., 2015a; 2015b; [Brégonzio-Rozier et al., 2015; 2016; Di](#)
460 [Biagio et al., 2014; 2017](#)).

461 CESAM is a multi-instrumented platform, equipped with twelve circular flanges to support its analytical
462 environment. Basic instrumentation comprises sensors to measure the temperature, pressure and relative
463 humidity within the chamber (two manometers MKS Baratrons (MKS, 622A and MKS, 626A) and a
464 HMP234 Vaisala® humidity and temperature sensor). The particle size distribution is routinely meas-
465 ured by a combination of (i) a scanning mobility particle sizer (SMPS, mobility diameter range 0.02–
466 0.88 µm), composed of a Differential Mobility Analyzer (DMA, TSI Inc. Model 3080) and a Conden-
467 sation Particle Counter (CPC, TSI Inc. Model 3772); (ii) a SkyGrimm optical particle counter (Grimm
468 Inc., model 1.129, optical equivalent diameter range 0.25–32 µm); and (iii) a WELAS optical particle
469 counter (PALAS, model 2000, optical equivalent diameter range 0.5–47 µm). Full details of operations
470 and data treatment of the particle counters are provided in [Di Biagio et al. \(2016, 2017\)](#).

471 **2.2. Filter sampling**

472 Three filter samples per top soil sample were collected on different types of substrate based on the anal-
473 ysis to [be performed](#). Sampling dedicated to the determination of the aerosol mass concentration by

474 gravimetric analysis and the measurement of the absorption coefficients by optical analysis was per-
475 formed on 47-mm quartz membranes (Pall Tissuquartz™, 2500 QAT-UP). Two samples were collected
476 in parallel. The first quartz membrane sample (“total”) was collected without a dedicated size cut-off
477 using an in-house built stainless steel sampler operated at 5 L min⁻¹. However, as detailed in Di Biagio
478 et al. (2016, 2017), the length of the sampling line from the intake point in the chamber to the filter en-
479 trance was 50 cm, yielding resulting in with a 50% cut-off of the transmission efficiency at 10.6 μm in
480 particle aerodynamic diameter. This fraction is therefore indicated as PM_{10.6} in the forthcoming follow-
481 ing discussion. The second quartz membrane sample was collected using a 4-stage DEKATI impactor
482 operated at the a flow rate of 10 L min⁻¹ to select the aerosol fraction of particles with aerodynamic
483 diameter smaller than 2.5 μm, indicated as PM_{2.5} here forth. Sampling for the analysis of the iron oxide
484 content was performed on polycarbonate filters (47-mm Nuclepore, Whatman; pore size of 0.4 μm)
485 using the same sample holder than as used for the total quartz filters, and therefore referring correspond-
486 ing to the PM_{10.6} mass fraction. Samples were collected at a flow rate of 6 L min⁻¹. All flow rates were
487 monitored by a thermal mass flow meter (TSI Inc., model 4140). These samples were also used to de-
488 termine the elemental composition (including Fe) and the fraction of iron oxides in the total mass.

489 2.3. The Multi-Wavelength Absorbance Analyzer (MWAA)

490 The aerosol absorption coefficient, $b_{\text{abs}}(\lambda)$, at 5 wavelengths ($\lambda = 375, 407, 532, 635$, and 850 nm) was
491 measured by *in situ* analysis of the quartz filter samples using the Multi-Wavelength Absorbance Ana-
492 lyzer (MWAA), described in detail in Massabò et al. (2013; 2015).

493 The MWAA performs a non-destructive scan of the quartz filters on at 64 different points, each ~ 1 mm²
494 wide. It measures the light transmission through the filter as well as backscattering at two different angles
495 (125° and 165°). This is necessary to constrain the multiple scattering effects occurring within the par-
496 ticle-filter system. The measurements are used as input of to a radiative transfer model (Hänel, 1987;
497 1994) as implemented by Petzold and Schönlinner (2004) for the Multi-Angle Absorption Photometry
498 (MAAP) measurements. In this model, a two stream approximation is applied (Coakley and Chylek,
499 1975), in which the fractions of hemispherical backscattered radiation with respect to the total scattering
500 for collimated and diffuse incident radiation are approximated on the basis of the Henyey-Greenstein
501 scattering phase function (Hänel, 1987). This approximation assumes a wavelength-independent asym-
502 metry parameter (g) set to 0.75, appropriate for mineral dust (Formenti et al., 2011; Ryder et al., 2013b).

503 The total uncertainty, including the effects of photon counting and the deposit inhomogeneity, on the
504 absorption coefficient measurement is estimated at 8% ([Petzold et al., 2004](#); [Massabò et al., 2013](#)).

505 **2.4. Gravimetric analysis**

506 The aerosol mass deposited on [the filters](#) (μg) was obtained by weighing the quartz filter before and after
507 sampling, after a period of 48 hours of conditioning in a room with controlled atmospheric conditions
508 (temperature, $T \sim 20 \pm 1$ °C; relative humidity, $\text{RH} \sim 50 \pm 5\%$). Weighing is performed with an analyt-
509 ical balance (Sartorius model MC5, precision of $1 \mu\text{g}$), and repeated three times to control the statistical
510 variability of the measurement. Electrostatic effects are removed by exposing the filters, prior weighing,
511 to a de-ionizer. The error ~~on~~[in](#) the measured mass is estimated at $1\theta \mu\text{g}$, including the repetition varia-
512 bility. The aerosol mass concentration ($\mu\text{g m}^{-3}$) is obtained by dividing the mass deposited on [the filter](#)
513 to the total volume of sampled air (m^3) obtained from the mass flowmeter measurements [\(+5%\)](#). [The](#)
514 [percent error on mass concentrations is estimated to 5%](#).

515 **2.5. Dust composition measurements**

516 **2.5.1. Elemental composition**

517 Elemental concentrations for the major constituents of mineral dust (Na, Mg, Al, Si, P, S, Cl, K, Ca, Fe,
518 Ti, Mn) were obtained by ~~a~~-Wavelength Dispersive X-ray ~~fluorescence~~[Fluorescence](#) (WD-XRF) of the
519 Nuclepore filters using a PW-2404 spectrometer by Panalytical. Excitation X-rays are produced by a
520 Coolidge tube ($I_{\text{max}} = 125$ mA, $V_{\text{max}} = 60$ kV) with a Rh anode; [the](#) primary X-ray spectrum can be
521 controlled by inserting filters (Al, at different thickness) between the anode and the sample. Each ele-
522 ment was analyzed three times, with specific conditions (voltage, tube filter, collimator, analyzing crys-
523 tal, and detector). Data collection was controlled by the SuperQ software provided with the instrument.
524 The elemental mass thickness ($\mu\text{g cm}^{-2}$), that is, the analyzed elemental mass per unit surface, was ob-
525 tained by comparing the elemental yields with a sensitivity curve measured in the same geometry on a
526 set of certified mono- or bi-elemental thin layer standards by Micromatter Inc. The certified uncertainty
527 ~~of~~[the](#) standard deposit ($\pm 5\%$) determines the lower limit ~~of~~[the](#) uncertainty ~~of~~[the](#) measured ele-
528 mental concentrations, which ranges ~~between~~ 8% and 10% depending on the [element](#) considered-~~ele-~~
529 [ment](#). Thanks to the uniformity of the aerosol deposit on the filters, the atmospheric elemental concen-
530 trations ($\mu\text{g m}^{-3}$) were calculated by multiplying the analyzed elemental mass thickness by the ratio
531 between the collection and analyzed surfaces of each sample (41 and 22 mm, respectively), then di-
532 ~~viding~~[ed](#) by the total sampled volume (m^3). Finally, concentrations of light-weight elements (atomic

533 number $Z < 19$) were corrected for the underestimation induced by the self-absorption of the emitted
534 soft X-rays inside aerosol particles according to Formenti et al. (~~2014~~2010).

535 Additional XRF analysis of the quartz filters ~~was~~ ~~has been~~ performed both in the PM_{10.6} and the PM_{2.5}
536 fractions, ~~so~~ to verify the absence of biases between the experiments dedicated to the determination of
537 particle composition ~~to~~ ~~and~~ those where the optical properties were measured.

538 2.6.2. Iron oxide content

539 The content and the mineralogical speciation of the iron oxides, also defined as free-iron, ~~that is i.e.~~, the
540 fraction of iron ~~which~~ ~~that~~ is not in the crystal lattice of silicates (Karickhoff and Bailey, 1973), was
541 determined by XANES (X-ray absorption near-edge structure) in the Fe K-range (K_{α} , 7112 eV) at the
542 SAMBA (Spectroscopies Applied to Materials based on Absorption) beamline at the SOLEIL synchro-
543 tron facility in Saclay, France (Briois et al., 2011). The position and shape of the K pre-edge and edge
544 peaks were analyzed as they depend on the oxidation state of iron and the atomic positions of the neigh-
545 boring ions, mostly O⁺ and OH⁻.

546 As in Formenti et al. (2014b), samples were mounted in an external setup mode. A Si(220) double-
547 crystal monochromator was used to produce a monochromatic X-ray beam, which was 3000 x 250 μm^2
548 in size at the focal point. The energy range was scanned from 6850 eV to 7800 eV at a step resolution
549 varying between 0.2 eV in proximity to the Fe-K absorption edge (at 7112 eV) to 2 eV in the extended
550 range. Samples were analyzed in fluorescence mode without prior preparation. One scan acquisition
551 lasted approximately 30 minutes, and was repeated three times to improve the signal-to-noise ratio.

552 The same analytical protocol was applied to five standards of Fe(III)-bearing minerals (**Table 1**), includ-
553 ing iron oxides (hematite, goethite) and silicates (illite, montmorillonite, nontronite). The standard spec-
554 tra were used to deconvolute the dust sample spectra to quantify the mineralogical status of iron. The
555 linear deconvolution ~~was~~, performed with the Athena IFEFFIT freeware analysis program (Ravel and
556 Newville, 2005). ~~This~~, provided ~~with~~ the proportionality factors, α_{i-} , representing the mass fraction of
557 elemental iron to be assigned to the i -th standard mineral. In particular, the values of α_{hem} and α_{goe}
558 represent the mass fractions of elemental iron that can be attributed to hematite and goethite, and $\alpha_{Fe\ ox}$
559 ($\alpha_{hem} + \alpha_{goe}$), the mass fraction of elemental iron that can be attributed to iron oxides.

560 2.6.3. Calculation of the iron oxide content

561 The measured elemental concentrations obtained by X-ray Fluorescence (XRF) are expressed in the
 562 form of elemental oxides and summed to estimate the total mineral dust mass concentration MC_{dust} ac-
 563 cording to the equation from Lide (1992)

564

$$565 \quad [MC_{dust}] = 1.12 \times \left\{ \begin{array}{l} 1.658[Mg] + 1.889[Al] + 2.139[Si] + 1.399[Ca] + 1.668[Ti] + 1.582[Mn] \\ + (0.5 \times 1.286 + 0.5 \times 1.429 + 0.47 \times 1.204)[Fe] \end{array} \right\} \quad (4)$$

566

567 The relative uncertainty ~~on~~ in MC_{dust} , estimated from the analytical error ~~in~~ the measured
 568 concentrations, does not exceed 6%. As it will be explained in the result section (paragraph 3.1), the
 569 values of MC_{dust} estimated from Equation 4 were found in excellent agreement with the measured
 570 gravimetric mass on the filters.

571 The fractional mass ratio (in percent) of elemental iron ($MR_{Fe\%}$) with respect to the total dust mass con-
 572 centration, MC_{dust} , is then calculated as

573

$$574 \quad MR_{Fe\%} = \frac{[Fe]}{[MC_{Dust}]} \times 100 \quad (5)$$

575

576 The mass concentration of iron oxides or free-iron ($MC_{Fe\ ox}$), representing the fraction of elemental iron
 577 in the form of hematite and goethite (Fe_2O_3 and $FeOOH$, respectively), is equal to

578

$$579 \quad MC_{Fe\ ox} = MC_{hem} + MC_{goe} \quad (6)$$

580

581 where MC_{hem} and MC_{goe} are the total masses of hematite and goethite. These can be calculated from the
 582 values α_{hem} and α_{goe} from XANES analysis, which represent the mass fractions of elemental iron at-
 583 tributed to hematite and goethite, as

584

$$585 \quad MC_{hem} = \frac{\alpha_{hem} \times [Fe]}{0.70} \quad (7.a)$$

$$MC_{goe} = \frac{\alpha_{goe} \times [Fe]}{0.63} \quad (7.b)$$

where the values of 0.70 and 0.63 represent the mass molar fractions of Fe in hematite and goethite, respectively. The relative errors of MC_{hem} and MC_{goe} are obtained from the uncertainties of the values of α_{hem} and α_{goe} from XANES analysis (less than 10%).

The mass ratio of iron oxides ($MR_{Fe\ ox\%}$) with respect to the total dust mass can then be calculated as

$$MR_{Fe\ ox\%} = MC_{Fe\ ox} \times MR_{Fe\ \%} \quad (8)$$

3. Experimental protocol

At the beginning of each experiment, the chamber was evacuated by to 10^{-4} - 10^{-5} hPa. Then, the reactor was filled with a mixture of 80% N₂ and 20% O₂ at a pressure slightly exceeding the current atmospheric pressure, in order to avoid contamination from ambient air. The experiments were conducted at ambient temperature and at a relative humidity <2%. As in Di Biagio et al. (2014; 2016,2017), dust aerosols were generated by mechanical shaking of the parent soils, previously sieved to < 1000 μm and dried at 100 °C for about 1 h to remove any residual humidity. About 15 g of soil was placed in a Buchner flask and shaken for about 30 min at 100 Hz by means of a sieve shaker (Retsch AS200). The dust particles produced by the mechanical shaking, mimicking the saltation processing that soils experience when eroded by strong winds, as were then injected in the chamber by flushing the flask with N₂ at 10 L min⁻¹ for about 10-15 min, whilst continuing shaking the soil. Di Biagio et al. (2014; 2017) have demonstrated the realism of the generation system concerning the composition and the size distribution of the generated dust with respect to the properties of mineral dust in the atmosphere.

The dust was injected for about 10-15 minutes, and left remained suspended in the chamber for approximately 120 min thanks to the 4-wheel fan located in the bottom of the chamber body. Previous measurements at the top and bottom of the chamber showed that the fan ensures a homogeneous distribution of the dust starting approximately 10 minutes after the end of the injection (Di Biagio et al., 2014).

613 To compensate for the air extracted from the chamber by sampling, a particle-free flow of N₂/O₂, regu-
614 lated in real time as a function of the total volume of sampled air, was re-injected in the chamber. To
615 avoid excessive dilution the flow was limited to 20 L min⁻¹. Two experiments per soil type were con-
616 ducted: a first experiment for sampling on the nuclepore polycarbonate filters (determination of the ele-
617 mental composition and the iron oxide fraction) and *in situ* measurements of the infrared optical con-
618 stants (Di Biagio et al., 20162017), and a second experiment [sampling](#) on total quartz filter and impactor
619 for the study of dust MAE presented in this paper.

620 **Figure 1** illustrates as typical example the time series of the aerosol mass concentration during the two
621 experiments conducted for the Libyan sample. The comparison demonstrates the repeatability of the dust
622 concentrations, both in absolute values and in temporal dynamics. It also shows that the mass concen-
623 trations decreased very rapidly by gravitational settling within the first 30 minutes of the experiment
624 (see also the discussion in Di Biagio et al., (20162017)), after which concentrations only decrease by
625 dilution. The filter sampling was started after this transient phase, and then continued through the end of
626 the experiments, in order to collect enough dust on [the filter membranes](#) for [subsequent the](#) chemical
627 analysis. Blank samples were collected before the start of the experiments by placing the [loaded filter](#)
628 holders [loaded with filter membranes](#) in line with the chamber and by flushing them for a few seconds
629 with air coming from the chamber.

630 At the end of each experimental series with a given soil sample, the chamber was manually cleaned in
631 order to remove carry-over caused by resuspension of particles deposited to the walls. Background con-
632 centrations of aerosols in the chamber vary between 0.5 and 2.0 µg m⁻³, i.e., a factor of 500 to 1000
633 below the operating conditions.

634 **34. Results and discussion**

635 The geographical location of the soil collection sites is shown in **Figure 2**, [whereas-and](#) the coordinates
636 are summarized in **Table 2**. [As-discussed-in-Di-Biagio-et-al.\(2016\),-the-selection-of-these-soils-and](#)
637 [sediments-was-governed-by-the-need-of-representing-the-major-arid-and-semi-arid-regions-worldwide,](#)
638 [the-need-of-taking-into-account-the-mineralogical-diversity-of-the-soil-composition-at-the-global-scale,](#)
639 [and-finally-by-their-availability-in-sufficient-quantities-for-injection-in-the-chamber.-When-doing-so,-we](#)
640 [obtained-a-set-of-twelve-samples-distributed-worldwide-but-mostly-in-Northern-and-Western-Africa](#)
641 [\(Libya, Algeria, Mali, Bodélé\) and the Middle East \(Saudi Arabia and Kuwait\). Individual samples from](#)
642 [the Gobi desert in Eastern Asia, the Namib Desert, the Strzelecki desert in Australia, the Patagonian](#)

643 ~~deserts in South America, and the Sonoran Desert in Arizona have also been investigated. The selection~~
644 ~~of these soils and sediments was made out of 137 individual top-soil samples collected in major arid and~~
645 ~~semi-arid regions worldwide and representing the mineralogical diversity of the soil composition at the~~
646 ~~global scale. As discussed in Di Biagio et al. (2017), this large sample set was reduced byto a set of 19~~
647 ~~samples representing the mineralogical diversity of the soil composition at the global scale and based on~~
648 ~~their availability in sufficient quantities for injection in the chamber. Because some of the experiments~~
649 ~~did not produce enough dust to perform good-quality optical measurements, in this paper we present a~~
650 ~~set of twelve samples distributed worldwide but mostly from Northern and Western Africa (Libya,~~
651 ~~Algeria, Mali, Bodélé) and the Middle East (Saudi Arabia and Kuwait). Individual samples from the~~
652 ~~Gobi desert in Eastern Asia, the Namib Desert, the Strzelecki desert in Australia, the Patagonian deserts~~
653 ~~in South America, and the Sonoran Desert in Arizona have were also been investigated.~~

654 **3.1. Elemental composition and iron oxide content**

655 A total of 41 filters including 15 polycarbonate filters (12 samples and 3 blanks) and 25 quartz filters
656 (12 for the total fraction, 10 for the fine fraction and 3 blanks) were collected for analysis.

657 The dust mass concentration found by gravimetric analysis varied between $50 \mu\text{g m}^{-3}$ and 5mg m^{-3} , in
658 relatively good agreement with the dust mass concentrations, MC_{dust} , from (Equation 4), based on ~~X-~~
659 ~~ray Ray fluorescence FluorescenceXRF analysisaAnalysis~~: the slope of the linear regression between
660 the calculated and the gravimetric values of MC_{dust} is 0.90 with $R^2 = 0.86$.

661 Di Biagio et al. (20162017) showed that clays are the most abundant mineral phases, together with quartz
662 and calcite, and that significant variability exists as function of the compositional heterogeneity of the
663 parent soils. Here we use the Fe/Ca and Si/Al elemental ratios obtained from ~~X-ray FluorescenceXRF~~
664 analysis to discriminate the origin of ~~used~~ dust samples. These ratios have been extensively used in the
665 past to discriminate the origin of African dust samples collected in the field (Chiapello et al., 1997;
666 Formenti et al., 2011; Formenti et al., 2014a). The values obtained during our experiments are reported
667 in **Table 3**. There is a very good correspondence between the values obtained for the Mali, Libya, ~~Al-~~
668 ~~geria, Mauritania~~ and (to a lesser extent) Morocco experiments to values found in environmental aerosol
669 samples by Chiapello et al. (1997) and Formenti et al. (2011; 2014a). ~~These authors indicate that dust~~
670 ~~from local erosion of Sahelian soils, such as from Mali, have Si/Al ratios in the range of 2-2.5 and Fe/Ca~~
671 ~~ratios in the range 3-20, depending on the time proximity to the erosion event. Dust from sources in the~~
672 ~~Sahara, such as Libya and Algeria, show Si/Al ratios in the range of 2-3 and Fe/Ca ratios in the range~~

673 0.7-3, whereas dust from Morocco has Si/Al ratios around 3 and Fe/Ca ratios around 0.4. The only major
674 difference is observed for the Bodélé experiment, for which the Fe/Ca ratio is enriched by a factor of 6
675 with respect to the values of 1 found during ~~to~~ the field observations (Formenti et al., 2011; ~~Formenti et~~
676 ~~al., 2014a~~). This could reflect the fact that the Bodélé aerosol in the chamber is generated from a sedi-
677 ment sample and not from a soil. As a matter of fact, the Bodélé sediment sample ~~is constituted~~ consists
678 of by a very fine powder which becomes very easily airborne. ~~Henceforth, and contrary to the soil sam-~~
679 ~~ples, this~~ This powder is likely to be injected in the chamber with little or no size fractionation. ~~Hence-~~
680 ~~forth, the aerosol generated from it~~ As a consequence, should have a closer ~~the~~ composition to the
681 original powder of the aerosol collected in the chamber could reflect more that of the parent sedimentary
682 soil than ~~the not the~~ other samples. On the other hand, Bristow et al. (2010) and Moskowitz et al. (2016)
683 showed ed that the iron content and speciation of the Bodélé sediments is very heterogeneous at the source
684 scale. For samples from areas other than ~~non-~~ northern African ~~samples~~, the largest variability is observed
685 for the Fe/Ca values, ranging from 0.1 to 8, whereas the Si/Al ratio varied only between 2.5 and 4.8. In
686 this case, values are available in the literature for comparison (e.g., Cornille et al., 1990; Reid et al.,
687 1994; Eltayeb et al., 2001; Lafon et al., 2006; Shen et al., 2007; Radhi et al., 2010; 2011; Formenti et
688 al., 2011; 2014a; Scheuvens et al., 2013, and references within). Values in the PM_{2.5} fraction are very
689 consistent with those obtained in the PM_{10.6}: their linear correlation has a slope of 1.03 (± 0.05) and a R^2
690 equal to 0.97, suggesting that the elemental composition is relatively size -independent.

691 The mass fraction of total Fe ($MC_{Fe\%}$ from Equation 5), also reported in **Table 3**, ranged from 2.8 (Na-
692 mibia) to 7.3% (Australia), ~~values found for the Namibia and the Australia samples, respectively.~~ This
693 These are in the range ~~is in good agreement with of~~ values reported in the literature, taking into account
694 that differences might be also due to the method (direct measurement/calculation) and/or the size fraction
695 over which the total dust mass concentration is estimated (Chiapello et al., 1997; Reid et al., 1994; 2003;
696 Derimian et al., 2008; Formenti et al., 2001; 2011; 2014a; Scheuvens et al., 2013). The agreement of
697 $MC_{Fe\%}$ values obtained by the XRF analysis of polycarbonate filters (Equation 5) and those obtained
698 from the XRF analysis of the quartz filters, normalized to the measured gravimetric mass is well within
699 10% (~~that is,~~ the percent error of each estimate). ~~An the e-~~ Exceptions are the samples ~~of from~~ Bodélé
700 and Algeria, for which the values obtained from the analysis of the quartz filters are significantly lower
701 than those obtained from the nuclepore filters (3.1% versus 4.1% for Bodélé and 4.3% versus 6.8% for
702 Algeria). We treat that as an additional source of error in the rest of the analysis, and add it to the total
703 uncertainty. In the PM_{2.5} fraction, the content of iron is more variable, ranging from 4.4% (Morocco) to

704 33.6% (Mali), showing a size dependence. A word of caution on this conclusion ~~as is that~~ the two esti-
705 mates are not necessarily consistent in the way that the total dust mass is estimated (from Equation 4 for
706 the PM_{10.6} fraction and by gravimetric weighing ~~for~~ the PM_{2.5}).

707 Finally, between 11 and 47% of iron in the samples can be attributed to iron oxides, in variable propor-
708 tions between hematite and goethite. The iron oxide fraction of total Fe in this study is ~~on~~ at the lower
709 end of the range (36-72%) estimated for field dust samples of Saharan/Sahelian origin (Formenti et al.
710 2014b). The highest value of Formenti et al. (2014b), obtained for a sample of locally-emitted dust col-
711 lected at the Banizoumbou station in the African Sahel, is anyhow in excellent agreement with the value
712 of 62% obtained for an experiment (not shown here) using a soil collected in the same area. Likewise,
713 the proportions between hematite and goethite (not shown) are reproduced, showing that goethite is more
714 abundant than hematite. The mass fraction of iron oxides ($MR_{Fe\ ox\%}$), estimated from Equation 8 and
715 shown in Table 3, ranges between 0.7% (Kuwait) ~~to~~ and 3.6% (Australia), which is in the range of
716 available field estimates (Formenti et al., 2014a; Moskowitz et al., 2016). For China, our value of $MR_{Fe\ ox\%}$
717 is lower by almost a factor of 3 ~~in comparison with~~ compared to that obtained on ~~the same~~ of the
718 same origin sample by Alfaro et al. (2004) (0.9% against 2.8%), whereas on a sample from Niger (~~how-~~
719 ~~ever~~ not considered in this study) our estimates and that by Alfaro et al. (2004) agree perfectly agree
720 (5.8%). A possible underestimate of the iron oxide fraction for samples other than those from the Sahara-
721 Sahel area could be due to the fact that - opposite to the experience of Formenti et al. (2014b) - the linear
722 deconvolutions of the XANES spectra were not always satisfactory (see Figure S1 in the supplementary).
723 This resulted in a significant residual between the observed and fitted XANES spectra. ~~Indeed~~ In fact,
724 the mineralogical reference for hematite is obtained from a soil from Niger (Table 1) and might not be
725 fully suitable for representing aerosols of different origins. Additional differences could arise from dif-
726 ferences in the size distributions of the generated aerosol. As a matter of fact, the number fraction of
727 particles in the size classes above 0.5 μm in diameter is are different in the dust aerosol generated in the
728 Alfaro et al. (2004) study with respect compared to ours. In the study by Alfaro et al. (2004), the number
729 fraction of particles is lowest in the 0.5-0.7 size class and highest between 1 and 5 μm . ~~On the contrary~~ In
730 contrast, in our study the number fraction is lowest in the 1-2 μm size range and highest between 0.5
731 and 0.7 μm . These differences could ~~yield~~ either be due to differences in the chemical composition
732 and/or ~~to a difference~~ in the total mass in the denominator of Equation 8.

733 **34.2. Spectral and size -variability of the mass absorption efficiency**

734 The spectral mass absorption efficiency (MAE) at 375, 407, 532, 635, and 850 nm for the PM_{10.6} and
735 the PM_{2.5} dust fractions are summarized in **Table 4** and displayed in **Figure 3**. Regardless of particle
736 size, the MAE values decrease with increasing wavelength (almost one order of magnitude between 375
737 and 850 nm), and display a larger variability at shorter wavelengths. The MAE values for the PM_{10.6}
738 range from $37 (\pm 3) 10^{-3} \text{ m}^2 \text{ g}^{-1}$ to $135 (\pm 11) 10^{-3} \text{ m}^2 \text{ g}^{-1}$ at 375 nm, and from $1.3 (\pm 0.1) 10^{-3} \text{ m}^2 \text{ g}^{-1}$ to 15
739 $(\pm 1) 10^{-3} \text{ m}^2 \text{ g}^{-1}$ at 850 nm. Maxima are found for the Australia and Algeria samples, whereas the minima
740 are for Bodélé and Namibia, respectively at 375 and 850 nm. In the PM_{2.5} fraction, the MAE values
741 range from $95 (\pm 8) 10^{-3} \text{ m}^2 \text{ g}^{-1}$ to $711 (\pm 70) 10^{-3} \text{ m}^2 \text{ g}^{-1}$ at 375 nm, and from $3.2 (\pm 0.3) 10^{-3} \text{ m}^2 \text{ g}^{-1}$ to 36
742 $(\pm 3) 10^{-3} \text{ m}^2 \text{ g}^{-1}$ at 850 nm. Maxima at both 375 and 850 nm are found for the Morocco sample, whereas
743 the minima are for Algeria and Namibia, respectively. The MAE values for mineral dust resulting from
744 this work are ~~in~~ relatively in good agreement with the estimates available in the literature (Alfaro et al.,
745 2004; Linke et al., 2006; Yang et al., 2009; Denjean et al., 2016), reported in **Table 5**. For the China
746 Ulah Buhn sample, Alfaro et al. (2004) reported $69.1 10^{-3}$ and $9.8 10^{-3} \text{ m}^2 \text{ g}^{-1}$ at 325 and 660 nm, respec-
747 tively. The former is lower than the value of $99 10^{-3} \text{ m}^2 \text{ g}^{-1}$ that we obtain by extrapolating our measure-
748 ment at 375 nm. Likewise, our values for the Morocco sample are higher than reported by Linke et al.
749 (2006) at 266 and 660 nm. Conversely, the agreement with the estimates of Yang et al. (2009) for mineral
750 dust locally re-suspended in Xianghe, near Beijing (China) is very good at all wavelengths between 375
751 and 880 nm. As expected, the MAE values for mineral dust resulting from this work are almost one
752 order of magnitude smaller than for other absorbing aerosols. For black carbon, MAE values are in the
753 range of $6.5\text{--}7.5 \text{ m}^2 \text{ g}^{-1}$ at 850 nm (Bond and Bergstrom, 2006; Massabò et al., 2016), and ~~vary-decrease~~
754 in a linear way with the logarithm of the ~~inversely with~~ wavelength. For brown carbon, the reported
755 MAE range between $2.3\text{--}7.0 \text{ m}^2 \text{ g}^{-1}$ at 350 nm (Chen and Bond, 2010; Kirchstetter et al., 2004; Massabò
756 et al., 2016), $0.05\text{--}1.2 \text{ m}^2 \text{ g}^{-1}$ at 440 nm (Wang et al., 2016) and $0.08\text{--}0.72 \text{ m}^2 \text{ g}^{-1}$ at 550 nm (Chen and
757 Bond, 2010).

758 The analysis of **Table 4** indicates that, at every wavelength, the MAE values in the PM_{2.5} fraction are
759 equal or higher than those for PM_{10.6}. The PM_{2.5}/PM_{10.6} MAE ratios reach values of 6 for the Mali sam-
760 ple, but are mostly in the range 1.5-3 for the ~~remaining-other~~ aerosols. The vValues decrease with wave-
761 length up to 635 nm, whereas at 850 nm they have values comparable to those at 375 nm. The observed
762 size ~~-~~dependence of the MAE values is consistent with the expected behavior of light absorption of
763 particles in the Mie and geometric optical regimes that ~~concern-are relevant for~~ the two size fractions.
764 Light ~~-~~absorption of particles of sizes s smaller or equivalent to the wavelength is proportional to their

765 bulk volume, whereas for larger particles absorption occurs on their surface only (Bohren and Huffmann,
766 1983). On the other hand, the size-resolved measurements of Lafon et al. (2006) show that the proportion
767 (by volume) of iron oxides might be higher in the coarse than in the fine fraction, which would counteract
768 the size-dependence behavior of MAE. To validate the observations, we calculated the spectrally-re-
769 solved MAE values in the two size fractions using the Mie code for homogeneous spherical particles
770 (Bohren and Huffmann, 1983) and the number size distribution estimated by (Di Biagio et al.,
771 [2016\(2017\)](#)) and averaged over the duration of filter sampling. We estimated the dust complex refractive
772 index as a volume-weighted average of a non-absorbing dust fraction having the refractive index of
773 kaolinite, [the](#) dominant mineral in our samples (see Di Biagio et al., [20162017](#)), from Egan et Hilgeman
774 (1979) and an absorbing fraction estimated from the mass fraction of iron oxides and having the refrac-
775 tive index of hematite (Bedidi and Cervelle, 1993). [The r](#)Results of this calculation indicate that the
776 observed size-[dependent](#) behavior is well reproduced at all wavelengths, even in the basic hypothesis
777 that the mineralogical composition does not change with size. The only exception is 850 nm, where at
778 times, PM_{2.5}/PM_{10.6} MAE ratio is much higher than expected theoretically. We attribute that to the rela-
779 tively high uncertainty affecting the absorbance measurements at this wavelength, where the signal-to-
780 noise ratio is low. Indeed, the two sets of values (MAE in the PM_{2.5} fraction and MAE in the PM_{10.6}
781 fraction) are not statistically different according to a two-pair t-test (0.01 and 0.05 level of confidence),
782 confirming that any attempt of differentiation [of](#) the size-[dependence](#) at this wavelength would require
783 a stronger optical signal.

784 The analysis of the spectral dependence, using [a-the](#) power-law function fit [as-\(from](#) Equation 2), pro-
785 vides [with](#) the values of the Angstrom Absorption Exponent (AAE), also reported in **Table 4**. Contrary
786 to the MAE values, there is no statistically significant size-[dependence](#) of the AAE values, ranging from
787 2.5 (± 0.2) to 4.1 (± 0.3), with an average of 3.3 (± 0.7), for the PM_{10.6} size fraction and between 2.6 (\pm
788 0.2) and 5.1 (± 0.4), with an average of 3.5 (± 0.8), for the PM_{2.5} fraction. Our values are in the range of
789 those published in the [open](#)-literature (Fialho et al., 2005; Linke et al., 2006; Müller et al., 2009; Petzold
790 et al., 2009; Yang et al., 2009; Weinzierl et al., 2011; Moosmüller et al., 2012; Denjean et al., 2016),
791 shown in **Table 5**. AAE values close to 1.0 are found for urban aerosols where fossil fuels combustion
792 is dominant, while AAE values for brown carbon (BrC) from incomplete combustion are in the range
793 3.5-4.2 (Yang et al., 2009; Chen et al., 2015; Massabò et al., 2016).

794 Finally, **Figure 4** shows correlations between [the](#) MAE values in the PM_{10.6} fraction (Figure [34.a](#)) and
795 in the PM_{2.5} fraction (Figure [34.b](#)) and the estimated percent mass fraction of iron and iron oxides

796 ($MC_{Fe\%}$ and $MC_{Fe\ ox\%}$), respectively. Regardless of the size fraction, ~~t~~he correlation between the MAE
797 values and the percent mass of total elemental iron are ~~satisfactory~~. ~~Higher higher correlations are ob-~~
798 ~~tained~~ at 375, 407 and 532 nm, ~~and in the $PM_{2.5}$ fraction, where a linear correlation with R^2 up to 0.94~~
799 ~~are obtained~~. Best correlations are obtained when forcing the intercept to zero, indicating that elemental
800 iron fully accounts for the measured absorption. At these wavelengths, linear correlations with the mass
801 fraction of iron oxides are ~~loose-low~~ in the $PM_{10.6}$ mass fraction (R^2 up to 0.38-0.62), but ~~again satisfac-~~
802 ~~tory~~ ~~higher~~ in the $PM_{2.5}$ fraction (R^2 up to 0.83-0.99), where, ~~whenever~~ ~~however~~, one should keep in mind
803 that they have been established only indirectly by considering the ratio of iron oxides to elemental iron
804 independent of size. At 660 and 850 nm, little or no robust correlations ~~are is~~ obtained, often ~~based~~ on
805 very few data points and with very low MAE values. It is noteworthy that, in both size fractions, the
806 linear correlation yields a non-zero intercept ~~is obtained~~, indicating ~~a contribution from minerals~~ other
807 ~~minerals but~~ ~~than~~ iron oxides ~~account to~~ ~~for~~ the measured absorption.

808 **4.5. Conclusive remarks**

809 In this paper, we reported ~~new~~ laboratory measurements of the shortwave mass absorption efficiency
810 (MAE) of mineral dust of different origins ~~and~~ as a function of size and wavelength in the 375-850 nm
811 range. ~~Results-Our results have been~~ ~~were~~ obtained in the CESAM simulation chamber using ~~generated~~
812 mineral dust ~~generated~~ from natural parent soils, ~~in combination with~~ ~~and~~ optical and gravimetric anal-
813 ysis on extracted samples.

814 Our results can be summarized as follows: at 375 nm, the MAE values are lower for the $PM_{10.6}$ mass
815 fraction (range 37-135 $10^{-3} \text{ m}^2 \text{ g}^{-1}$) than for the $PM_{2.5}$ ~~fraction~~ (range 95-711 $10^{-3} \text{ m}^2 \text{ g}^{-1}$), and vary oppo-
816 site to wavelength as λ^{-AAE} , where AAE (Angstrom Absorption Exponent) averages between 3.3-3.5
817 regardless of size fraction. These results deserve some ~~conclusive-concluding~~ comments:

- 818 • The size ~~-~~dependence, ~~yielding-characterized by~~ significantly higher MAE values in the fine
819 fraction ($PM_{2.5}$) than ~~for the in the bulk~~ ($PM_{10.6}$) aerosol, indicates that light ~~-~~absorption by min-
820 eral dust can be important even during atmospheric transport over heavil~~y~~ polluted regions, ~~when~~
821 ~~where~~ dust concentrations are significantly lower than at emission. This can be shown by com-
822 paring the aerosol absorption optical depth (AAOD) at 440 nm for China, a well-known mixing
823 region of mineral dust and pollution (e.g., Yang et al., 2009; Laskin et al., 2014; Wang et al.,
824 2013), ~~as well as offshore western Africa where large urban centers are downwind of dust~~
825 ~~transport areas~~ (Petzold et al., 2011). Laskin et al. (2014) reports that the average AAOD in ~~China~~

826 ~~the area~~ is of the order of 0.1; for carbonaceous absorbing aerosols (sum of black and brown
827 carbon; [Andreae and Gelencsér, 2006](#)). This is lower or comparable to the AAOD of 0.17 and
828 0.11 at 407 nm (~~fine and~~ total ~~and fine~~ mass fractions, respectively) that we ~~obtain~~ derive by a
829 simple calculation ($AAOD = MAE \times MC_{dust} \times H$), ~~where from~~ MAE ~~are the~~ values estimated in
830 this study, ~~(MC_{dust})~~ the dust mass concentrations typically observed in ~~the area~~ urban area of
831 [Beijing](#) during dust storms (Sun et al., ~~2004~~2005), and H , a scale height factor of 1 km).

832 • The spectral variability of the dust MAE values, represented by the AAE parameter, is equal in
833 the PM_{2.5} and PM_{10.6} mass fractions. This suggests that, for a given size distribution, the possible
834 variation of dust composition with size ~~does~~ not affect in a significant way the spectral behavior
835 of the absorption properties. Our average value for AAE is 3.3 ± 0.7 , higher than for black carbon,
836 but in the same range ~~than as~~ light-absorbing organic (brown) carbon. As a result, depending on
837 the environment, there can be some ambiguity in apportioning the AAOD based on spectral de-
838 pendence. Bahadur et al. (2012) and Chung et al. (2012) couple the AAE and the spectral de-
839 pendence of the total AOD (~~and/or its scattering fraction only~~) to overcome this problem. Still,
840 Bahadur et al. (2012) show that there is an overlap in the scatterplots of the spectral dependence
841 of the scattering and absorption fractions of the AOD based on ~~an~~ analysis of ground-based re-
842 mote sensing data for mineral dust, urban, and non-urban fossil fuel over California. A closer
843 look ~~should be taken at~~ observations in mixing areas where biomass burning ~~aerosols may~~
844 have different chemical composition and/or mineral dust has heavy loadings ~~should be given~~ in
845 order to generalize the clear separation observed in the spectral dependences of mineral dust and
846 biomass burning (Bahadur et al., 2012). This aspect is relevant to the development of remote
847 sensing ~~retrievals~~ of light-absorption ~~by~~ aerosols from space, and their assimilation in climate
848 models (Torres et al., 2007; Buchard et al., 2015; Hammer et al., 2016).

849 • There is an important sample-to-sample variability in our dataset of MAE values for mineral dust
850 aerosols. At 532 nm, our ~~estimated average~~ MAE ~~values~~ ~~average to are~~ at $34 \pm 14 \text{ m}^2 \text{ g}^{-1}$ and 78
851 $\pm 70 \text{ m}^2 \text{ g}^{-1}$ in the PM_{10.6} and PM_{2.5} mass fractions, respectively. Figure 3, showing the correlation
852 with the estimated mass fraction of elemental iron and iron oxides, suggests that this variability
853 could be related to the regional differences of the mineralogical composition of the parent soils.
854 These observations lead to ~~different considerations~~ ~~further conclusions~~. To start with, our study
855 reinforces the need for regionally-resolved representation of the light-absorption properties of

856 mineral dust in order to improve the representation of its effect on climate. As a matter of fact,
857 the natural variability of the absorption properties that we obtain from our study is in the range
858 50-100%, even when we limit ourselves to smaller spatial scales, for example those ~~of from~~ north
859 Africa (samples from Libya, Algeria, Mali and Bodélé). ~~This is far above the $\pm 5\%$ sensitivity~~
860 ~~factor used by Solmon et al. (2008) to vary the single scattering albedo (as a proxy of absorption)~~
861 ~~of mineral dust over western Africa, and to show how this could drastically change the climate~~
862 ~~response in the region. As a comparison, Solmon et al. (2008) showed that varying the single~~
863 ~~scattering albedo of mineral dust over western Africa by $\pm 5\%$, that is, varying the co-albedo (or~~
864 ~~absorption) by 45% (0.1 ± 0.045) could drastically change the climate response in the region.~~

865 The question is then “how to represent this regional variability?” ~~As Like~~ Moosmüller et al.
866 (2012) ~~and Engelbrecht et al. (2016)~~, we found that elemental iron is a very good proxy for the
867 MAE, especially in the PM_{2.5} fraction, where iron-bearing absorbing minerals (hematite, goe-
868 thite, illite, smectite clays) ~~would beare~~ more concentrated. In the coarse fraction, Ca-rich min-
869 erals, quartz, and feldspars could also play a role, and that could result in the observed lower~~ed~~
870 correlation (although adding a term proportional to elemental Ca does not ~~ameliorate-improve~~
871 the ~~correlation-result~~ in the present study). The correlation of the spectral MAE values with the
872 iron oxide fraction is satisfactory but rather noisy, also owing to some uncertainty in the quanti-
873 fication of iron oxides from X-Ray ~~Absorption-absorption~~ measurements. In this case, the inter-
874 cept is significantly different from zero, again indicating that a small but ~~clear-distinct~~ fraction
875 of absorption is due to minerals other than iron oxides. There are contrasting results on this topic:
876 Alfaro et al. (2004) found an excellent correlation between MAE and the iron oxide content,
877 whereas Klaver et al. (2011) found that the single scattering albedo (representing the capacity of
878 an aerosol population to absorb light ~~with respect in relation~~ to extinction) was almost independ-
879 ent on the mass fraction of iron oxides. Moosmüller et al. (2012) disagreed, pointing out ~~to~~ the
880 uncertainty in the correction procedure of the measurement of absorption by Klaver et al. (2011).
881 As a matter of fact, Klaver et al. (2011) and Alfaro et al. (2004) used the same correction proce-
882 dure. It is more likely that the lack of correlation found in Klaver et al. (2011) is due to the fact
883 that ~~other~~ minerals ~~other~~ than iron oxides contribute to absorption, in particular at their working
884 wavelength (567 nm), where the absorption efficiency of iron oxides starts to weaken. Clearly,
885 the linear correlation between elemental iron in mineral dust and its light-absorption properties

886 could ease the application and validation of climate models that [are](#) now starting [to include in-](#)
887 [cluding](#) the representation of the mineralogy (Perlwitz et al., 2015a; 2015b; Scanza et al., 2015).
888 Also, [they-this](#) would facilitate detecting source regions based on remote sensing of dust absorp-
889 tion in the UV-VIS spectral region (e.g., Hsu et al., 2004). However, such a quantitative relation-
890 ship cannot [be](#) uniquely determined from these studies, including the present one, which use
891 different ways of estimating elemental iron, iron oxides, and the total dust mass. A more robust
892 estimate should be obtained [fromby estimating](#) the imaginary parts of the complex refractive
893 indices associated [to-with](#) these measurements of absorption, and their dependence on the min-
894 eralological composition.

895 **Author contributions**

896 L. Caponi, P. Formenti, D. Massabò, P. Prati, C. Di Biagio, and J. F. Doussin designed the chamber
897 experiments and discussed the results. L. Caponi and C. Di Biagio [realized-conducted](#) the experiments
898 with contributions by M. Cazaunau, E. Pangui, P. Formenti, and J.F. Doussin. L. Caponi, D. Massabò
899 and P. Formenti performed the full data analysis with contributions by C. Di Biagio, P. Prati and J.F.
900 Doussin. L. Caponi, P. Formenti and S. Chevaillier performed the XRF measurements. P. Formenti and
901 G. Landrot performed the XAS measurements. D. Massabò performed the MWAA and the gravimetric
902 measurements. M. O. Andreae, K. Kandler, T. Saeed, S. Piketh, D. Seibert, and E. Williams collected
903 the soil samples used for experiments. L. Caponi, P. Formenti, D. Massabò and P. Prati wrote the man-
904 uscript with comments from all co-authors.

905 **Acknowledgements**

906 [The RED-DUST project was supported by the French national programme LEFE/INSU, by the EC](#)
907 [within the I3 project “Integration of European Simulation Chambers for Investigating Atmospheric Pro-](#)
908 [cesses” \(EUROCHAMP 2020, grant agreement n. 730997\), by the Institut Pierre Simon Laplace \(IPSL\),](#)
909 [and by OSU-EFLUVE \(Observatoire des Sciences de l’Univers-Enveloppes Fluides de la Ville à l’Ex-](#)
910 [obiologie\) through dedicated research funding. This work has received funding from the European Un-](#)
911 [ion’s Horizon 2020 research and innovation programme through the EUROCHAMP-2020 Infrastructure](#)
912 [Activity under grant agreement no. 730997. It was supported by the French national programme](#)
913 [LEFE/INSU, by the OSU-EFLUVE \(Observatoire des Sciences de l’Univers-Enveloppes Fluides de la](#)
914 [Ville à l’Exobiologie\) through dedicated research funding, by the CNRS-INSU by supporting CESAM](#)
915 [as national facility, and by the project of the TOSCA program of the CNES \(Centre National des Etudes](#)

916 [Spatales](#)). C. Di Biagio was supported by the CNRS via the Labex L-IPSL. M. O. Andreae was sup-
917 ported [by funding from King Saud University and the Max Planck Society](#)~~by the Max Society and by~~
918 [King Saud University](#). The mobility of researchers between Italy and France was supported by the PICS
919 programme MedMEx of the CNRS-INSU. The authors acknowledge the CNRS-INSU for supporting
920 CESAM as national facility. K. Kandler acknowledges support from the Deutsche Forschungsgemein-
921 schaft (DFG grant KA 2280/2-1). [The authors strongly thank the LISA staff who participated in the](#)
922 [collection of the soil samples from Patagonia and the Gobi desert used in this study, and the two anon-](#)
923 [ymous reviewers for useful comments on the manuscript. P. Formenti thanks Dr. Hans Moosmüller](#)
924 [\(Desert Research Institute, Reno, Nevada\) for providing with fruitful](#) ~~elements~~[suggestions for-of im-](#)
925 [provement and discussion to the paper.](#)

926 **References**

- 927 Alfaro, S. C., Lafon, S., Rajot, J. L., Formenti, P., Gaudichet, A., and Maille, M., Iron oxides and light
928 absorption by pure desert dust: An experimental study, *J. Geophys. Res. Atmos.*, 109, D08208,
929 doi:10.1029/2003JD004374, 2004.
- 930 [Andreae, M. O., and Gelencsér, A., Black carbon or brown carbon? The nature of light-absorbing car-](#)
931 [bonaceous aerosols: *Atmos. Chem. Phys.*, 6, 3131-3148, 2006.](#)
- 932 [Anderson, T. L. and Ogren, J. A., Determining aerosol radiative properties using the TSI 3563 integrat-](#)
933 [ing nephelometer, *Aerosol. Sci. Technol.*, 29, 57–69, 1998.](#)
- 934 [Andrews, E., Sheridan, P. J., Fiebig, M., McComiskey, A., Ogren, J. A., Arnott, P., Covert, D., Elleman,](#)
935 [R., Gasparini, R., Collins, D., Jonsson, H., Schmid, B., and Wang J., Comparison of methods](#)
936 [for deriving aerosol asymmetry parameter, *J. Geophys. Res.*, 111, D05S04,](#)
937 [doi:10.1029/2004JD005734, 2006.](#)
- 938 [Arnott, W., Hamasha, K., Moosmüller, H., Sheridan, P. J., and Ogren, J. A., Towards aerosol light-](#)
939 [absorption measurements with a 7 wavelength aethalometer: Evaluation with a photoacoustic](#)
940 [instrument and 3 wavelength nephelometer, *Aerosol Sci Tech.*, 39\(1\), 17–29, 2005.](#)
- 941 Bahadur, R., P. S. Praveen, Y. Xu, and V. Ramanathan, Solar absorption by elemental and brown carbon
942 determined from spectral observations, *PNAS*, 109(43), 17366-17371, 2012.
- 943 Balkanski, Y., Schulz, M., Claquin, T., and Guibert, S., Re-evaluation of Mineral aerosol radiative forc-
944 ing suggests a better agreement with satellite and AERONET data, *Atmos. Chem. Phys.*, 7, 81–
945 95, doi:10.5194/acp-7-81-2007, 2007.
- 946 Bedidi, A., and Cervelle B., Light scattering by spherical particles with hematite and goethitelike optical
947 properties: Effect of water impregnation, *J. Geophys. Res.*, 98(B7), 11941–11952,
948 doi:10.1029/93JB00188, 1993.
- 949 Bond, T.C. and Bergstrom, R.W., Light absorption by carbonaceous particles: an investigative review.
950 *Aerosol Sci. Technol.* 40, 27e67, 2006.

- 951 Boucher, O., Randall, D., Artaxo, P., Bretherton, C., Feingold, G., Forster, P., Kerminen, V.-M., Kondo,
952 Y., Liao, H., Lohmann, U., Rasch, P., Satheesh, S.K., Sherwood, S., Stevens B., and Zhang X.
953 Y., Clouds and Aerosols. In: Climate Change 2013: The Physical Science Basis. Contribution of
954 Working Group I to the Fifth Assessment Report of the Intergovernmental Panel on Climate
955 Change [Stocker, T.F., D. Qin, G.-K. Plattner, M. Tignor, S.K. Allen, J. Boschung, A. Nauels,
956 Y. Xia, V. Bex and P.M. Midgley (eds.)]. Cambridge University Press, Cambridge, United King-
957 dom and New York, NY, USA, 2013.
- 958 Brégonzio-Rozier, L., F. Siekmann, C. Giorio, E. Pangui, S. B. Morales, B. Temime-Roussel, Aline
959 Gratien, V. Michoud, S. Ravier, A. Tapparo, A. Monod, Jean-Francois Doussin, Gaseous prod-
960 ucts and secondary organic aerosol formation during long term oxidation of isoprene and meth-
961 acrolein, *Atmos. Chem. Phys.*, 15, 2953-2968, 2015.
- 962 Brégonzio-Rozier L., C. Giorio, F. Siekmann, E. Pangui, S. B. Morales, B. Temime-Roussel, A. Gratien,
963 V. Michoud, M. Cazaunau, H. L. DeWitt, A. Tapparo, A. Monod and J.-F. Doussin, Secondary
964 Organic Aerosol formation from isoprene photooxidation during cloud condensation-evaporation
965 cycles, *Atmospheric Chemistry and Physics*, 16: 1747-1760, 2016.
- 966 Bristow, C. S., Hudson-Edwards, K. A., and Chappell, A.: Fertilizing the Amazon and equatorial Atlan-
967 tic with West African dust, *Geophys. Res. Lett.*, 37, L14807, 10.1029/2010GL043486, 2010.
- 968 Buchard, V., da Silva, A. M., Colarco, P. R., Darmenov, A., Randles, C. A., Govindaraju, R., Torres,
969 O., Campbell, J., and Spurr, R.: Using the OMI aerosol index and absorption aerosol optical
970 depth to evaluate the NASA MERRA Aerosol Reanalysis, *Atmos. Chem. Phys.*, 15, 5743–5760,
971 doi:10.5194/acp-15-5743-2015, 2015.
- 972 Chen, L.-W.A., Chow, J.C., Wang, X.L., Robles, J.A., Sumlin, B.J., Lowenthal, D.H., Zimmermann, R.,
973 Watson, J.G., Multi-wavelength optical measurement to enhance thermal/optical analysis for car-
974 bonaceous aerosol, *Atmos. Meas. Tech.* 8, 451-461, 2015.
- 975 Chen, Y. and Bond, T. C., Light absorption by organic carbon from wood combustion, *Atmos. Chem.*
976 *Phys.*, 10:1773–1787, 2010.
- 977 [Chiapello, I., G. Bergametti, B. Chatenet, P. Bousquet, F. Dulac, and E. Santos Soares, Origins of Afri-
978 can dust transported over the northeastern tropical Atlantic., *J. Geophys. Res.*, 102\(D12\), 13701-
979 13709, 1997.](#)
- 980 Chiapello, I., Dust Observations and Climatology, in P. Knippertz and J.-B.W. Stuut (eds.), *Mineral
981 Dust: A Key Player in the Earth System*, DOI 10.1007/978-94-017-8978-3__7, ©Springer Sci-
982 enceCBusiness Media, Dordrecht, 2014.
- 983 Chung, C. E., V. Ramanathan, and D. Decremer, Observationally constrained estimates of carbonaceous
984 aerosol radiative forcing, *PNAS*, 109(29), 11624-11629, 2012.
- 985 Coakley, J.A. and Chylek, P., The two-stream approximation in radiative transfer: Including the angle
986 of incident radiation, *J. Atmos. Sci.* 32, 409 – 418, 1975.
- 987 Colarco, P. R., O. B. Toon, O. Torres, and F. J. Rasch, Determining the UV imaginary part of refractive
988 index of Saharan dust particles from TOMS data and a three dimensional model of dust transport,
989 *J. Geophys. Res.*, 107(D16), 10.1029/2001JD000903, 2002.

- 990 [Collaud Coen, M., Weingartner, E., Apituley, A., Ceburnis, D., Fierz-Schmidhauser, R., Flentje, H.,](#)
991 [Henzing, J.S., Jennings, S.G., Moerman, M., Petzold, A., Schmid, O., Baltensperger, U., Mini-](#)
992 [mizing light absorption measurement artifacts of the Aethalometer: evaluation of five correction](#)
993 [algorithms, Atmos. Meas. Tech. 3, 457-474, 2010.](#)
- 994 Denjean, C., Paola Formenti, Benedicte Picquet-Varrault, Edouard Pangui, Pascal Zapf, Y. Katrib, C.
995 Giorio, A. Tapparo, A. Monod, B. Temime-Roussel, P. Decorse, C. Mangeney, Jean-Francois
996 Doussin, Relating hygroscopicity and optical properties to chemical composition and structure
997 of secondary organic aerosol particles generated from the ozonolysis of α -pinene, Atmos. Chem.
998 Phys., 15, 3339-3358, 2015a.
- 999 Denjean, C., Paola Formenti, Benedicte Picquet-Varrault, Marie Camredon, Edouard Pangui, Pascal
1000 Zapf, Katrib, Y., Giorio, C., Tapparo, A., Temime-Roussel, B., Monod, A., Bernard Aumont,
1001 Jean-Francois Doussin, Aging of secondary organic aerosol generated from the ozonolysis of α -
1002 pinene: effects of ozone, light and temperature, Atmos. Chem. Phys., 15, 883-897,
1003 doi:10.5194/acp-15-883-2015, 2015b.
- 1004 Denjean, C., Cassola, F., Mazzino, A., Triquet, S., Chevaillier, S., Grand, N., Bourriane, T., Mom-
1005 boisse, G., Sellegri, K., Schwarzenbock, A., Freney, E., Mallet, M., and Formenti, P., Size distri-
1006 bution and optical properties of mineral dust aerosols transported in the western Mediterranean,
1007 Atmos. Chem. Phys., 15, 21607–21669, doi:10.5194/acpd-15-21607-2015, 2015c.
- 1008 Denjean, C., *et al.*, Size distribution and optical properties of African mineral dust after intercontinental
1009 transport, J. Geophys. Res. Atmos., 121, 7117–7138, doi:10.1002/2016JD024783, 2016.
- 1010 Derimian, Y., A. Karnieli, Y. J. Kaufman, M. O. Andreae, T. W. Andreae, O. Dubovik, W. Maenhaut,
1011 and I. Koren: The role of iron and black carbon in aerosol light absorption. Atmos. Chem. Phys.,
1012 8, 3623–3637, (2008).
- 1013 Di Biagio, C., Formenti P., Styler S. A., Pangui E., and Doussin J.-F., Laboratory chamber measurements
1014 of the longwave extinction spectra and complex refractive indices of African and Asian mineral
1015 dusts, Geophys. Res. Lett., 41, 6289-6297, doi:10.1002/2014GL060213, 2014.
- 1016 [Di Biagio, C., Formenti, P., Balkanski, Y., Caponi, L., Cazaunau, M., Pangui, E., Journet, E., Nowak, S., Ca-](#)
1017 [quineau, S., Andreae, M. O., Kandler, K., Saeed, T., Piketh, S., Seibert, D., Williams, E., and Doussin,](#)
1018 [J.-F.: Global scale variability of the mineral dust long-wave refractive index: a new dataset of in situ](#)
1019 [measurements for climate modeling and remote sensing, Atmos. Chem. Phys., 17, 1901-1929,](#)
1020 [doi:10.5194/acp-17-1901-2017, 2017.](#)
- 1021 [Di Biagio, C., Formenti, P., Balkanski, Y., Caponi, L., Cazaunau, M., Pangui, E., Journet, E., Nowak,](#)
1022 [S., Caquineau, S., Andreae, M. O., Kandler, K., Saeed, T., Piketh, S., Seibert, D., Williams, E.,](#)
1023 [and Doussin, J.-F.: Global scale variability of the mineral dust longwave refractive index: a new](#)
1024 [dataset of in situ measurements for climate modelling and remote sensing, Atmos. Chem. Phys.](#)
1025 [Discuss., doi:10.5194/acp-2016-616, in review, 2016.](#)
- 1026 Dubovik, O., B. N. Holben, T. F. Eck, A. Smirnov, Y. J. Kaufman, M. D. King, D. Tanre, and I. Slutsker,
1027 Variability of absorption and optical properties of key aerosol types observed in worldwide lo-
1028 cations, J. Atmos. Sci., 59, 590–608, 2002.
- 1029 Egan, W. G. and Hilgeman, T. W.: Optical Properties of Inhomogeneous Materials: Applications to
1030 Geology, Astronomy, Chemistry, and Engineering, Academic Press, 235 pp., 1979.

- 1031 [Engelbrecht, J. P., Moosmüller, H., Pincock, S., Jayanty, R. K. M., Lersch, T., and Casuccio, G.: Technical note:](#)
1032 [Mineralogical, chemical, morphological, and optical interrelationships of mineral dust re-suspensions,](#)
1033 [Atmos. Chem. Phys., 16, 10809-10830, doi:10.5194/acp-16-10809-2016, 2016.](#)
- 1034 Fialho, P., A.D.A. Hansen, R.E. Honrath, Absorption coefficients by aerosols in remote areas: a new
1035 approach to decouple dust and black carbon absorption coefficients using seven-wavelength Ae-
1036 thalometer data, *J. Aeros. Sci.*, 36, 267–282, 2005.
- 1037 ~~[Filep, Á., Ajtai, T., Utry, N., Pintér, M., Nyilas, T., Takács, S., Máté, Z., Gelencsér, A., Hoffer, A.,](#)~~
1038 ~~[Schnaiter, M., Bozóki, Z., and Szabó, G., Absorption spectrum of ambient aerosol and its corre-](#)~~
1039 ~~[lation with size distribution in specific atmospheric conditions after a Red Mud Accident, *Aero-*](#)~~
1040 ~~[sol Air Qual. Res.](#)~~ 13, 49–59, 2013.
- 1041 Formenti, P., S. Nava, P. Prati, S. Chevaillier, A. Klaver, S. Lafon, F. Mazzei, G. Calzolari, and M. Chiari,
1042 Self-attenuation artifacts and correction factors of light element measurements by X-ray analysis:
1043 Implication for mineral dust composition studies, *J. Geophys. Res.*, 115, D01203,
1044 doi:10.1029/2009JD012701, 2010.
- 1045 Formenti, P., Rajot, J. L., Desboeufs, K., Saïd, F., Grand, N., Chevaillier, S., and Schmechtig, C., Air-
1046 borne observations of mineral dust over western Africa in the summer Monsoon season: spatial
1047 and vertical variability of physico-chemical and optical properties, *Atmos. Chem. Phys.*, 11,
1048 6387–6410, doi:10.5194/acp-11-6387-2011, 2011.
- 1049 Formenti, P., Caquineau, S., Desboeufs, K., Klaver, A., Chevaillier, S., Journet, E. and Rajot, J. L.,
1050 Mapping the physico-chemical properties of mineral dust in western Africa: mineralogical com-
1051 position, *Atmos. Chem. Phys.*, 14, 10663–10686, doi:10.5194/acp-14-10663-2014, 2014a.
- 1052 Formenti, P., Caquineau, S., Chevaillier, S., Klaver, A., Desboeufs, K., Rajot, J. L., Belin, S. and Briois,
1053 V.: Dominance of goethite over hematite in iron oxides of mineral dust from western Africa:
1054 quantitative partitioning by X-ray Absorption Spectroscopy, *J. Geophys. Res.*, 2014b.
- 1055 Hammer, M. S., Martin, R. V., van Donkelaar, A., Buchard, V., Torres, O., Ridley, D. A., and Spurr, R.
1056 J. D.: Interpreting the ultraviolet aerosol index observed with the OMI satellite instrument to
1057 understand absorption by organic aerosols: implications for atmospheric oxidation and direct ra-
1058 diative effects, *Atmos. Chem. Phys.*, 16, 2507-2523, doi:10.5194/acp-16-2507-2016, 2016.
- 1059 Hänel, G., Radiation budget of the boundary layer: Part II. Simultaneous measurement of mean solar
1060 volume absorption and extinction coefficients of particles, *Beitr. Phys. Atmos.* 60, 241-247,
1061 1987.
- 1062 Hänel, G., Optical properties of atmospheric particles: complete parameter sets obtained through polar
1063 photometry and an improved inversion technique, *Appl. Opt.* 33, 7187-7199, 1994.
- 1064 Harrison, R.M., Beddows, D.C.S., Jones, A.M., Calvo, A., Alves, C., and Pio, C., An evaluation of some
1065 issues regarding the use of aethalometers to measure woodsmoke concentrations, *Atmos. Envi-*
1066 *ron.* 80, 540e548, 2013.
- 1067 Haywood, J. M., P. N. Francis, M. D. Glew, and J. P. Taylor, Optical properties and direct radiative
1068 effect of Saharan dust: A case study of two Saharan outbreaks using data from the U. K. Met.
1069 Office C-130, *J. Geophys. Res.*, 106, 18,417–18,430, 2001.
- 1070 Haywood, J., Francis, P., Osborne, S., Glew, M., Loeb, N., Highwood, E., Tanré, D., Myhre, G., For-
1071 menti, P., and Hirst, E., Radiative properties and direct radiative effect of Saharan dust measured

- 1072 by the C-130 aircraft during Saharan Dust Experiment (SHADE). 1: Solar spectrum, *J. Geophys.*
1073 *Res.*, 108(D18), 8577, doi:10.1029/2002JD002687, 2003.
- 1074 Hsu, N. C., S.-C. Tsay, M. D. King, and J. R. Herman, Aerosol Properties Over Bright-Reflecting Source
1075 Regions, *IEEE Transactions Geos. Remote Sens.*, 42, 557-569, 2004.
- 1076 IPCC 2013, Climate Change 2013: The Scientific Basis, Summary for Policymakers, Working Group I
1077 Contribution to the Fifth Assessment Report of the Intergovernmental Panel on Climate Change,
1078 edited by: Stocker, T. F., Qin, D., Plattner, G.-K., Tignor, M. M. B., Allen, S. K., Boschung, J.,
1079 Nauels, A., Xia, Y., Bex, V., Midgley, P. M., Cambridge University Press, Cambridge, UK, 2013.
- 1080 Journet, E., Balkanski, Y., and Harrison, S. P., A new data set of soil mineralogy for dust-cycle model-
1081 ing, *Atmos. Chem. Phys.*, 14, 3801-3816, doi:10.5194/acp-14-3801-2014, 2014.
- 1082 Kandler, K., Benker, N., Bundke, U., Cuevas, E., Ebert, M., Knippertz, P., Rodriguez, S., Schütz, L.,
1083 and Weinbruch, S.: Chemical composition and complex refractive index of Saharan Mineral Dust
1084 at Izaña, Tenerife (Spain) derived by elec-tron microscopy, *Atmos. Environ.*, 41, 8058-8074,
1085 10.1016/j.atmosenv.2007.06.047, 2007.
- 1086 Kandler, K., Schütz, L., Deutscher, C., Hofmann, H., Jäckel, S., Knippertz, P., Lieke, K., Massling, A.,
1087 Schladitz, A., Wein-zierl, B., Zorn, S., Ebert, M., Jaenicke, R., Petzold, A., and Weinbruch, S.,
1088 Size distribution, mass concentration, chemical and mineralogical composition, and derived op-
1089 tical parameters of the boundary layer aerosol at Tinfou, Morocco, during SAMUM 2006, *Tellus*,
1090 61B, 32-50, 10.1111/j.1600-0889.2008.00385.x, 2009.
- 1091 Kandler, K., Lieke, K., Benker, N., Emmel, C., Küpper, M., Müller-Ebert, D., Ebert, M., Scheuvsens, D.,
1092 Schladitz, A., Schütz, L., and Weinbruch, S.: Electron microscopy of particles collected at Praia,
1093 Cape Verde, during the Saharan Mineral dust experiment: particle chemistry, shape, mixing state
1094 and complex refractive index, *Tellus*, 63B, 475-496, 10.1111/j.1600-0889.2011.00550.x, 2011.
- 1095 Karickhoff, S. W. and Bailey, G. W., Optical absorption spectra of clay minerals, *Clays Clay Min.*, 21,
1096 59-70, 1973.
- 1097 Kirchstetter, T.W., Novakok, T., Hobbs, P.V., Evidence that the spectral dependence of light absorption
1098 by aerosols is affected by organic carbon, *J. Geophys. Res.* 109, D21208, 2004.
- 1099 Klaver, A., Formenti, P., Caquineau, S., Chevaillier, S., Ausset, P., Calzolari, G., Osborne, S., Johnson,
1100 B., Harrison, M., and Dubovik, O., Physico-chemical and optical properties of Sahelian and
1101 Saharan mineral dust: in situ measurements during the GERBILS campaign, *Q. J. R. Meteorol.*
1102 *Soc.*, DOI:10.1002/qj.889, 2011.
- 1103 Knippertz, P., and J.-B. W. Stuut (eds.), *Mineral Dust: A Key Player in the Earth System*, DOI
1104 10.1007/978-94-017-8978-3__1, Springer ScienceCBusiness Media Dordrecht, 2014.
- 1105 ~~Lack, D. A., and Langridge, J. M., On the attribution of black and brown carbon light absorption using~~
1106 ~~the Angström exponent, *Atmos. Chem. Phys.* 13, 10535-10543, 2013.~~
- 1107 Lafon, S., J. Rajot, S. Alfaro, and A. Gaudichet, Quantification of iron oxides in desert aerosol, *Atmos.*
1108 *Environ.*, 38, 1211-1218, 2004.
- 1109 Lafon, S., Sokolik, I.N., Rajot, J.L., Caquineau, S., Gaudichet, A., Characterization of iron oxides in
1110 mineral dust aerosols: Implications for light absorption, *J. Geophys. Res.* 111, D21207,
1111 DOI:10.1029/2005JD007016, 2006.

- 1112 Laskin, J., Laskin, A., Nizkorodov, S. A., Roach, P., Eckert, P., Gilles, M. K., Wang, B., Lee, H. J., and
1113 Hu, Q., Molecular Selectivity of Brown Carbon Chromophores, *Environ. Sci. Technol.*, 48,
1114 12047–12055, 2014.
- 1115 Lau, K. M., K. M. Kim, Y. C. Sud, and G. K. Walker, A GCM study of the response of the atmospheric
1116 water cycle of West Africa and the Atlantic to Saharan dust radiative forcing, *Ann. Geophys.*,
1117 27, 4023–4037, doi:10.5194/angeo-27-4023-2009, 2009.
- 1118 Lazaro, F. J., L. Gutiérrez, V. Barrón, and M. D. Gelado, The speciation of iron in desert dust collected
1119 in Gran Canaria (Canary Islands): Combined chemical, magnetic and optical analysis, *Atmos.*
1120 *Environ.*, 42(40), 8987-8996, 2008.
- 1121 ~~Lewis, K., Arnott, W. P., Moosmüller, H., Wold, C. E., Strong spectral variation of biomass smoke light~~
1122 ~~absorption and single scattering albedo observed with a novel dual wavelength photoacoustic~~
1123 ~~instrument, *J. Geophys. Res.* 113, D16203, 2008.~~
- 1124 ~~Liao, H., and Seinfeld, J.H., Radiative forcing by mineral dust aerosols: Sensitivity to key variables, *J.*~~
1125 ~~*Geophys. Res.*, 103, 31,637-31,645, 1998.~~
- 1126 Lide, D. R., *CRC Handbook of Chemistry and Physics 1991 – 1992*, CRC Press, Boca Raton, Fla., 1992.
- 1127 Linke, C., Möhler, O., Veres, A., Mohácsi, A., Bozóki, Z., Szabó, G., and Schnaiter, M., Optical prop-
1128 erties and mineralogical composition of different Saharan mineral dust samples: a laboratory
1129 study, *Atmos. Chem. Phys.*, 6, 3315–3323, 2006.
- 1130 Loeb, N. G., and W. Su, Direct Aerosol Radiative Forcing Uncertainty Based on a Radiative Perturbation
1131 Analysis, *J. Climate*, 23, 5288, 2010.
- 1132 Massabó, D., Bernardoni, V., Bove, M.C., Brunengo, A., Cuccia, E., Piazzalunga, A., Prati, P., Valli,
1133 G., Vecchi, R., A multi-wavelength optical set-up for the characterization of carbonaceous par-
1134 ticulate matter, *J. Aerosol Sci.* 60, 34-46, 2013.
- 1135 Massabó, D., Caponi, L., Bernardoni, V., Bove, M.C., Brotto, P., Calzolari, G., Cassola, F., Chiari, M.,
1136 Fedi, M.E., Fermo, P., Giannoni, M., Lucarelli, F., Nava, S., Piazzalunga, A., Valli, G., Vecchi,
1137 R., Prati, P., Multi-wavelength optical determination of black and brown carbon in atmospheric
1138 aerosols, *Atmos. Environ.*, 108, 1-12, 2015.
- 1139 Massabò, D., Caponi, L., Bove, M.C., Prati, P., Brown carbon and thermal-optical analysis: A correction
1140 based on optical multi-wavelength apportionment of atmospheric aerosols, *Atmos. Environ.*,
1141 125, 119-125. doi: 10.1016/j.atmosenv.2015.11.011, 2016.
- 1142 ~~McConnell, C.L., E. J. Highwood, H. Coe, P. Formenti, B. Anderson, S. Osborne, S. Nava, and G. Chen,~~
1143 ~~Seasonal variations of the physical and optical characteristics of Saharan dust: results from the~~
1144 ~~Dust Outflow and Deposition to the Ocean (DODO) Experiment, *J. Geophys. Res.*, 113,~~
1145 ~~<http://dx.doi.org/10.1029/2007JD009606>, 2008.~~
- 1146 ~~McConnell, C. L., P. Formenti, E. J. Highwood, and M. A. J. Harrison, Using aircraft measurements to~~
1147 ~~determine the refractive index of Saharan dust during the DODO Experiments, *Atmos. Chem.*~~
1148 ~~*Phys.*, 10(6), 3081-3098, 2010.~~
- 1149 Miller, R.L., Tegen, I. and Perlwitz, J.P., Surface radiative forcing by soil dust aerosols and the hydro-
1150 logic cycle, *J. Geophys. Res.*, 109, D04203, doi:10.1029/2003JD004085, 2004.

- 1151 Miller, R.L., Knippertz, P., Garcia-Pardo, C.P., Perlwitz, J.P., and Tegen, I., Impact of dust radiative
1152 forcing upon climate, *Mineral Dust*, 327-357, Springer Netherlands, 2014.
- 1153 Ming, Y, Ramaswamy V, and G. Persad, Two opposing effects of absorbing aerosols on global mean
1154 precipitation, *Geophys. Res. Lett.* 37, L13701. doi:10.1029/2010GL042895, 2010.
- 1155 Moosmüller, H., Chakrabarty, R. K., and W. P. Arnott, Aerosol light absorption and its measurement:
1156 A review, *J. Quant. Spectr. Rad. Trans.*, 110, 844–878, 2009.
- 1157 Moosmüller, H., Engelbrecht, J. P., Skiba, M., Frey, G., Chakrabarty, R.K., and Arnott, W.P., Single
1158 scattering albedo of fine mineral dust aerosols controlled by iron concentration, *J. Geophys. Res.*,
1159 117, D11210, doi:10.1029/2011JD016909, 2012.
- 1160 Moskowicz, B. M., R. L. Reynolds, H. L. Goldstein, T. S. Berquó, R. F. Kokaly, and C. S. Bristow, Iron
1161 oxide minerals in dust-source sediments from the Bodélé Depression, Chad: Implications for
1162 radiative properties and Fe bioavailability of dust plumes from the Sahara, *Aeolian Research*, 22,
1163 93-106, 2016.
- 1164 Müller, T., Schladitz, A., Massling, A., Kaaden, N., Kandler, K., and Wiedensohler, A., Spectral absorp-
1165 tion coefficients and imaginary parts of refractive indices of Saharan dust during SAMUM-1,
1166 *Tellus B*, 61, 79–95, doi:10.3402/tellusb.v61i1.16816, 2009.
- 1167 Patterson, E. M., D. A. Gillette, and B. H. Stockton, Complex index of refraction between 300 and 700
1168 nm for Saharan aerosol, *J. Geophys. Res.*, 82, 3153– 3160, 1977.
- 1169 Pérez C., S. Nickovic, G. Pejanovic, J. M. Baldasano, and E. Özsoy, Interactive dust-radiation modeling:
1170 a step to improve weather forecasts, *J. Geophys. Res.*, 111:D16206.
1171 doi:10.1029/2005JD0067172006, 2006.
- 1172 Perlwitz J., R. Miller, Cloud cover increase with increasing aerosol absorptivity—a counterexample to
1173 the conventional semi-direct aerosol effect, *J. Geophys. Res.*, 115:D08203.
1174 doi:10.1029/2009JD012637, 2010.
- 1175 Perlwitz, J. P., Pérez García-Pando, C., and R. L. Miller, Predicting the mineral composition of dust
1176 aerosols – Part 1: Representing key processes, *Atmos. Chem. Phys.*, 15, 11593-11627,
1177 doi:10.5194/acp-15-11593-2015, 2015a.
- 1178 Perlwitz, J. P., Pérez García-Pando, C., and R. L. Miller, Predicting the mineral composition of dust
1179 aerosols – Part 2: Model evaluation and identification of key processes with observations, *Atmos.*
1180 *Chem. Phys.*, 15, 11629-11652, doi:10.5194/acp-15-11629-2015, 2015b.
- 1181 Petzold, A., Schönlinner, M., Multi-angle absorption photometry - a new method for the measurement
1182 of aerosol light absorption and atmospheric black carbon, *J. Aerosol Sci.* 35, 421-441, 2004.
- 1183 Petzold, A., Rasp, K., Weinzierl, B., Esselborn, M., Hamburger, T., Dornbrack, A., Kandler, K., Schütz,
1184 L., Knippertz, P., Fiebig, M., Virkkula, A., Saharan dust absorption and refractive index from
1185 aircraft-based observations during SAMUM 2006, *Tellus B* 61: 118–130, 2009.
- 1186 [Petzold, A., Veira, A., Mund, S., Esselborn, M., Kiemle, C., Weinzierl, B., Hamburger, T., Ehret, G.,
1187 Lieke, K., and Kandler, K.: Mixing of mineral dust with urban pollution aerosol over Dakar
1188 \(Senegal\): impact on dust physico-chemical and radiative properties, *Tellus*, 63B, 619-634, doi:
1189 \[10.1111/j.1600-0889.2011.00547.x\]\(#\), 2011.](#)

- 1190 [Petzold, A., Onasch, T., Keabian, P. and Freedman, A., Interecomparison of a Cavity Attenuated Phase](#)
1191 [Shift-based extinction monitor \(CAPS PMex\) with an integrating nephelometer and a filter-based](#)
1192 [absorption monitor, Atmos. Meas. Tech., 6, 1141–1151, doi:10.5194/amt-6-1141-2013, 2013.](#)
- 1193 Ravel, B., and M. Newville, ATHENA, ARTEMIS, HEPHAESTUS: data analysis for X-ray absorption
1194 spectroscopy using IFEFFIT, *J. Synchrotron Radiation* 12, 537–541,
1195 doi:10.1107/S0909049505012719, 2005.
- 1196 Ryder, C. L., Highwood, E. J., Rosenberg, P. D., Trembath, J., Brooke, J. K., Bart, M., Dean, A., Crosier,
1197 J., Dorsey, J., Brindley, H., Banks, J., Marsham, J. H., McQuaid, J. B., Sodemann, H., and Wash-
1198 ington, R., , Optical properties of Saharan dust aerosol and contribution from the coarse mode as
1199 measured during the Fennec 2011 aircraft campaign, *Atmos. Chem. Phys.*, 13, 303-325,
1200 doi:10.5194/acp-13-303-2013, 2013a.
- 1201 Ryder, C. L., E. J. Highwood, T. M. Lai, H. Sodemann, and J. H. Marsham, Impact of atmospheric
1202 transport on the evolution of microphysical and optical properties of Saharan dust, *Geophys. Res.*
1203 *Lett.*, 40, 2433–2438, doi:10.1002/grl.50482, 2013b.
- 1204 Scanza, R. A., Mahowald, N., Ghan, S., Zender, C. S., Kok, J. F., Liu, X., Zhang, Y., and Albani, S.:
1205 Modeling dust as component minerals in the Community Atmosphere Model: development of
1206 framework and impact on radiative forcing, *Atmos. Chem. Phys.*, 15, 537–561, doi:10.5194/acp-
1207 15-537-2015, 2015.
- 1208 [Sertsu, S. M., and Sánchez, P. A., Effects of Heating on Some Changes in Soil Properties in Relation to](#)
1209 [an Ethiopian Land Management Practice, Soil Sci. Soc. Am. J., 42, 940–944, 1978.](#)
- 1210 Shen, Z. X., J. J. Cao, R. Arimoto, R. J. Zhang, D. M. Jie, S. X. Liu, and C. S. Zhu, Chemical composition
1211 and source characterization of spring aerosol over Horqin sand land in northeastern China, *J.*
1212 *Geophys. Res.*, 112, D14315, doi:10.1029/2006JD007991, 2007.
- 1213 Sinyuk, A., O. Torres, and O. Dubovik, Combined use of satellite and surface observations to infer the
1214 imaginary part of refractive index of Saharan dust, *Geophys. Res. Lett.*, 30(2), 1081,
1215 doi:10.1029/2002GL016189, 2003.
- 1216 Slingo, A., et al., Observations of the impact of a major Saharan dust storm on the atmospheric radiation
1217 balance, *Geophys. Res. Lett.*, 33, L24817, doi:10.1029/2006GL027869, 2006.
- 1218 [Sokolik, I., and Toon, O., Incorporation of mineralogical composition into models of the radiative prop-](#)
1219 [erties of mineral aerosol from UV to IR wavelengths, J. Geophys. Res., 104\(D8\), 9423–9444,](#)
1220 [1999.](#)
- 1221 Solmon, F., Mallet, M., Elguindi, N., Giorgi, F., Zakey, A. and Konaré, A., Dust aerosol impact on
1222 regional precipitation over western Africa, mechanisms and sensitivity to absorption properties,
1223 *Geophys. Res. Lett.*, 35, L24705, doi:10.1029/2008GL035900, 2008.
- 1224 [Sun J., Zhang, M., and Liu, T., Spatial and temporal characteristics of dust storms in China and its](#)
1225 [surrounding regions, 1960–1999: Relations to source area and climate, J. Geophys. Res.,](#)
1226 [106\(D10\), 10325–10333, 2001.](#)
- 1227 [Sun, Y., G. Zhuang, Y. Wang, X. Zhao, J. Li, Z. Wang, and Z. An \(2005\), Chemical composition of dust](#)
1228 [storms in Beijing and implications for the mixing of mineral aerosol with pollution aerosol on the](#)
1229 [pathway, J. Geophys. Res., 110, D24209, doi:10.1029/2005JD006054.](#)

- 1230 Tegen, I., and Lacis, A. A., Modeling of particle size distribution and its influence on the radiative prop-
1231 erties of mineral dust aerosol, *J. Geophys. Res.*, doi:10.1029/95JD03610, 1996.
- 1232 Torres, O., A. Tanskanen, B. Veihelmann, C. Ahn, R. Braak, P. K. Bhartia, P. Veefkind, and P. Levelt,
1233 Aerosols and surface UV products from Ozone Monitoring Instrument observations: An over-
1234 view, *J. Geophys. Res.*, 112, *D24S47*, doi:10.1029/2007JD008809, 2007.
- 1235 ~~Utry, N., Ajtai, T., Filep, Á., Pintér, M., Hoffer, A., Bozóki, Z., and Szabó, G., Mass specific optical~~
1236 ~~absorption coefficient of HULIS aerosol measured by a four-wavelength photoacoustic spec-~~
1237 ~~trometer at NIR, VIS and UV wavelengths, *Atmos. Environ.* 69, 321–324, 2013.~~
- 1238 Utry, N., Ajtai, T., Filep, Á., Pintér, M., Tombacz, E., Bozóki, Z., and Szabó, G., Correlations between
1239 absorption Ångström exponent (AAE) of wintertime ambient urban aerosol and its physical and
1240 chemical properties, *Atmos. Environ.* 91, 52–59, 2014.
- 1241 Xian, P., Seasonal migration of the ITCZ and implications for aerosol radiative impact. PhD thesis,
1242 Columbia University, 2008.
- 1243 Vinoj, V., Rasch, P. J., Wang, H., Yoon, J.-H., Ma, P.-L., Landu, K., and Singh, B., Short-term modu-
1244 lation of Indian summer monsoon rainfall by West Asian dust, *Nat. Geosci.*, 7, 308–313,
1245 doi:10.1038/ngeo2107, 2014.
- 1246 Wang, J., J. F. Doussin, S. Perrier, E. Perraudin, Y. Katrib, E. Pangui, and B. Picquet-Varrault, Design
1247 of a new multi-phase experimental simulation chamber for atmospheric photosimulation, aerosol
1248 and cloud chemistry research, *Atmos. Meas. Tech.*, 4, 2465–2494, 2011.
- 1249 Wang, L., Z. Li, Q. Tian, Y. Ma, F. Zhang, Y. Zhang, D. Li, K. Li, and L. Li, Estimate of aerosol
1250 absorbing components of black carbon, brown carbon, and dust from ground-based remote sens-
1251 ing data of sun-sky radiometers, *J. Geophys. Res. Atmos.*, 118, 6534–6543,
1252 doi:10.1002/jgrd.50356, [20132016](#).
- 1253 Weinzierl, B., et al., , Microphysical and optical properties of dust and tropical biomass burning aerosol
1254 layers in the Cape Verde region—an overview of the airborne in situ and lidar measurements
1255 during SAMUM-2, *Tellus B*, 63(4), 589–618, 2011.
- 1256 Yang, M., Howell, S.G., Zhuang, J., Huebert, B.J., Attribution of aerosol light absorption to black car-
1257 bon, brown carbon, and dust in China - interpretations of atmospheric measurements during
1258 EAST-AIRE, *Atmos. Chem. Phys.* 9, 2035e2050, 2009.
- 1259 Zhang, X. Y., Y. Q. Wang, X. C. Zhang, W. Guo, T. Niu, S. L. Gong, Y. Yin, P. Zhao, J. L. Jin, and M.
1260 Yu, Aerosol monitoring at multiple locations in China: contributions of EC and dust to aerosol
1261 light absorption, *Tellus B*, 60(4), 647–656, 2008.
- 1262 Zhao, C., Liu, X., Ruby Leung, L., and Hagos, S.: Radiative impact of mineral dust on monsoon precip-
1263 itation variability over West Africa, *Atmos. Chem. Phys.*, 11, 1879–1893, 10.5194/acp-11-1879-
1264 2011, 2011.
- 1265

1266 **Table captions**

1267 **Table 1.** Characteristics of the standards used for the quantification of the iron oxides in the XAS anal-
1268 ysis.

1269 **Table 2.** ~~Summary-Geographical~~ of information on the soil samples used in this work.

1270 **Table 3.** Chemical characterisation of the dust aerosols in PM_{10.6} and PM_{2.5} (in parentheses) size frac-
1271 tions. Columns 3 and 4 ~~report-give~~ the Si/Al and Fe/Ca elemental ratios obtained from X-Ray Fluores-
1272 cence analysis. The uncertainty of ~~fa~~ each individual value is estimated to be 10%. Column 5 ~~reports~~
1273 ~~shows~~ $MR_{Fe\%}$, the fractional mass of elemental iron with respect to the total dust mass concentration
1274 (uncertainty 10%). Column 5 reports $MR_{Fe\%}$, the mass fraction of iron oxides with respect to the total
1275 dust mass concentration (uncertainty 15%). For PM_{2.5} the determination of the Si/Al ratio is impossible
1276 due to the composition of the filter ~~medium-membranes~~ (quartz).

1277 **Table 4.** Mass absorption efficiency (MAE, $10^{-3} \text{ m}^2 \text{ g}^{-1}$) and Ångström Absorption Exponent (AAE) in
1278 the PM_{10.6} and PM_{2.5} size fractions. Absolute errors are in brackets.

1279 **Table 5.** Mass absorption efficiency (MAE, $10^{-3} \text{ m}^2 \text{ g}^{-1}$) and Ångström Absorption Exponent (AAE) ~~of~~
1280 ~~from the~~ literature data discussed in the paper

1281

1282 **Figure captions**

1283 **Figure 1.** Time series of aerosol mass concentration in the chamber for ~~the~~ two companion experiments
1284 (Libyan ~~dust-sample~~). Experiment 1 (top panel) was dedicated to the determination of the chemical
1285 composition (including iron oxides) by sampling on polycarbonate filters. Experiment 2 (bottom panel)
1286 was dedicated to the determination of the absorption optical properties by sampling on quartz filters.

1287 **Figure 2.** Locations (red stars) of the soil and sediment samples used to generate dust aerosols.

1288 **Figure 3.** Spectral dependence of the MAE values for the samples investigated in this study in the PM_{10.6}
1289 (left) and in the PM_{2.5} (right) mass fractions.

1290 **Figure 4.** Illustration of the links between the MAE values and the dust chemical composition found in
1291 this study. Left column, from top to bottom: linear regression between ~~the~~ MAE values ~~between-in the~~
1292 ~~range from~~ 375 ~~toand~~ 850 nm and the fraction of elemental iron ~~with-respect-to-relative to~~ the total dust
1293 mass ($MR_{Fe\%}$) in the PM_{10.6} fraction; Middle column: same as left column but ~~respect-tofor~~ the mass

1294 fraction of iron oxides [relative](#) to the total dust mass ($MR_{Fe\ ox\%}$) in the PM_{10.6} size fraction; Right column:
1295 same as left column but in the PM_{2.5} size fraction.
1296

1297 **Table 1.** Characteristics of the standards used for the quantification of the iron oxides in the XAS anal-
 1298 ysis.

Standard	Stoichiometric Stoichiometric Formula	Origin
Illite of Puy	$(\text{Si}_{3.55}\text{Al}_{0.45})(\text{Al}_{1.27}\text{Fe}_{0.36}\text{Mg}_{0.44})\text{O}_{10}(\text{OH})_2(\text{Ca}_{0.01}\text{Na}_{0.01}\text{K}_{0.53}\text{X}(\text{I})_{0.12})$	Puy, France
Goethite	$\text{FeO} \cdot \text{OH}$	Minnesota
Hematite	Fe_2O_3	Niger
Montmorillonite	$(\text{Na},\text{Ca})_{0.3}(\text{Al},\text{Mg})_2\text{Si}_4\text{O}_{10}(\text{OH})_2 \cdot n(\text{H}_2\text{O})$	Wyoming
Nontronite	$\text{Na}_{0.3}\text{Fe}_2(\text{Si},\text{Al})_4\text{O}_{10}(\text{OH})_2 \cdot n\text{H}_2\text{O}$	Pennsylvania

1299

1300

1301

1302 **Table 2.** Geographical information on the soil samples used in this work.

Geographical area	Sample	Desert area	Geographical coordinates
Sahara	Morocco	East of Ksar Sahli	31.97°N, 3.28°W
	Libya	Sebha	27.01°N, 14.50°E
	Algeria	Ti-n-Tekraouit	23.95°N, 5.47°E
Sahel	Mali	Dar el Beida	17.62°N, 4.29°W
	Bodélé	Bodélé depression	17.23°N, 19.03°E
Middle East	Saudi Arabia	Nefud	27.49°N, 41.98°E
	Kuwait	Kuwaiti	29.42°N, 47.69°E
Southern Africa	Namibia	Namib	21.24°S, 14.99°E
Eastern Asia	China	Gobi	39.43°N, 105.67°E
North America	Arizona	Sonoran	33.15 °N, 112.08°W
South America	Patagonia	Patagonia	50.26°S, 71.50°W
Australia	Australia	Strzelecki	31.33°S, 140.33°E

1303

1304

Table 3. Chemical characterisation of the dust aerosols in PM_{10.6} and PM_{2.5} (in parentheses) size fractions. Columns 3 and 4 give the Si/Al and Fe/Ca elemental ratios obtained from X-Ray Fluorescence analysis. The uncertainty of each individual value is estimated to be 10%. Column 5 shows $MR_{Fe\%}$, the fractional mass of elemental iron with respect to the total dust mass concentration (uncertainty 10%). Column 5 reports $MR_{Fe-ox\%}$, the mass fraction of iron oxides with respect to the total dust mass concentration (uncertainty 15%). For PM_{2.5} the determination of the Si/Al ratio is impossible due to the composition of the filter- membranes (quartz)

~~Chemical characterisation of the dust aerosols in PM_{10.6} and PM_{2.5} (in parentheses) size fractions. Columns 3 and 4 report the Si/Al and Fe/Ca elemental ratios obtained from X-Ray Fluorescence analysis. The uncertainty on each individual value is estimated to be 10%. Column 5 reports $MR_{Fe\%}$, the fractional mass of elemental iron with respect to the total dust mass concentration (uncertainty 10%). Column 5 reports $MR_{Fe-ox\%}$, the mass fraction of iron oxides with respect to the total dust mass concentration (uncertainty 15%). For PM_{2.5} the determination of the Si/Al ratio is impossible due to the composition of the filter medium.~~

Geographical area	Sample	Si/Al	Fe/Ca	MC _{Fe%}	MC _{Fe-ox%}
Sahara	Morocco	3.12 (---)	0.24 (0.28)	3.6 (4.4)	1.4 (1.8)
	Libya	2.11 (---)	1.19 (1.12)	5.2 (5.6)	3.1 (3.4)
	Algeria	2.51 (---)	3.14 (4.19)	6.6 (5.4)	2.7 (2.2)
Sahel	Mali	3.03 (---)	2.99 (3.67)	6.6 (33.6)	3.7 (18.7)
	Bodélé	5.65 (---)	12.35 (----)	4.1 (----)	0.7 (----)
Middle East	Saudi Arabia	2.95 (---)	0.29 (0.27)	3.8 (5.1)	2.6 (3.5)
	Kuwait	3.15 (---)	0.89 (1.0)	5.0 (13.6)	1.5 (4.2)
Southern Africa	Namibia	3.41 (---)	0.11 (0.10)	2.4 (6.9)	1.1 (3.1)
Eastern Asia	China	2.68 (---)	0.77 (0.71)	5.8 (13.6)	0.9 (2.5)
North America	Arizona	3.30 (---)	0.95 (----)	5.3 (----)	1.5 (----)
South America	Patagonia	4.80 (---)	4.68 (4.64)	5.1 (----)	1.5 (---)
Australia	Australia	2.65 (---)	5.46 (4.86)	7.2 (11.8)	3.6 (5.9)

1320

1321

1322 **Table 4.** Mass absorption efficiency (MAE, $10^{-3} \text{ m}^2 \text{ g}^{-1}$) and Ångström Absorption Exponent (AAE) in
 1323 the $\text{PM}_{10.6}$ and $\text{PM}_{2.5}$ size fractions. Absolute errors are in brackets.

		PM_{10.6}					
Geographical area	Sample	375 nm	407 nm	532 nm	635 nm	850 nm	AAE
Sahara	Morocco	--- (---)	--- (---)	--- (---)	--- (---)	--- (---)	--- (---)
	Libya	89 (11)	75 (9)	30 (5)	--- (---)	--- (---)	3.2 (0.3)
	Algeria	99 (10)	80 (10)	46 (7)	16 (3)	15 (3)	2.5 (0.3)
Sahel	Mali	--- (---)	103 (18)	46 (12)	--- (---)	--- (---)	--- (---)
	Bodélé	37 (4)	25 (3)	13 (2)	6 (1)	3 (1)	3.3 (0.3)
Middle East	Saudi Arabia	90 (9)	79 (8)	28 (3)	6 (1)	4 (1)	4.1 (0.4)
	Kuwait	--- (---)	--- (---)	--- (---)	--- (---)	--- (---)	2.8 (0.3)
Southern Africa	Namibia	52 (7)	49 (7)	13 (3)	5 (2)	1 (2)	4.7 (0.5)
Eastern Asia	China	65 (8)	58 (7)	32 (4)	8 (2)	7 (2)	3 (0.3)
North America	Arizona	130 (15)	99 (12)	47 (7)	21 (4)	13 (4)	3.1 (0.3)
South America	Patagonia	102 (11)	80 (9)	29 (4)	17 (2)	10 (2)	2.9 (0.3)
Australia	Australia	135 (15)	121 (13)	55 (7)	26 (4)	14 (3)	2.9 (0.3)

1324
 1325

PM _{2.5}							
Geographical area	Sample	375 nm	407 nm	532 nm	635 nm	850 nm	AAE
Sahara	Morocco	107 (13)	88 (11)	34 (6)	14 (3)	15 (4)	2.6 (0.3)
	Libya	132(17)	103 (14)	33 (7)	--- (---)	--- (---)	4.1 (0.4)
	Algeria	95(8)	71 (11)	37 (7)	12 (5)	12 (5)	2.8 (0.3)
Sahel	Mali	711 (141)	621 (124)	227 (78)	--- (---)	--- (---)	3.4 (0.3)
	Bodelé	--- (---)	--- (---)	--- (---)	--- (---)	--- (---)	--- (---)
Middle East	Saudi Arabia	153 (18)	127 (15)	42 (7)	8 (4)	6 (4)	4.5 (0.5)
	Kuwait	270 (100)	324 (96)	--- (---)	54 (52)	--- (---)	3.4 (0.3)
Southern Africa	Namibia	147 (36)	131 (32)	31 (21)	6 (16)	3 (15)	5.1 (0.5)
Eastern Asia	China	201 (30)	176 (26)	89 (17)	14 (10)	23 (10)	3.2 (0.3)
North America	Arizona	--- (---)	--- (---)	--- (---)	--- (---)	--- (---)	--- (---)
South America	Patagonia	--- (---)	--- (---)	--- (---)	--- (---)	--- (---)	2.9 (0.3)
Australia	Australia	335 (39)	288 (33)	130 (19)	57 (11)	36 (9)	2.9 (0.3)

1326
1327

1328 **Table 5.** Mass absorption efficiency (MAE, $10^{-3} \text{ m}^2 \text{ g}^{-1}$) and Ångström Absorption Exponent (AAE)
 1329 [from the efliterature data](#) discussed in the paper

Geo- graphical area	Sample	266 nm	325 nm	428 nm	532 nm	660 nm	880 nm	106 4 nm	AAE
	Morocco*								2.25– 5.13
	Morocco, PM _{2.5} [‡]								2.0–6.5
Sa- hara	Morocco, submicron [#]	1100			60			30	4.2
	Egypt, submicron [#]	810			20				5.3
	Tunisia [§]		83			11			
	Saharan, transported ^μ								2.9 ± 0.2
	Saharan, transported (PM ₁₀) [°]			37	27 ^{%%}	15 ^{%%%}			2.9
	Saharan, transported (PM ₁) [°]			60	40 ^{%%}	30 ^{%%%}			2.0
Sahel	Niger [§]		124			19			
East- ern Asia	China [§]		69			10			
	China ^{&}		87 ^{&}	50 ^{&&&}	27 ^{&&&}	13	1		3.8
Ara- bian Penin- sula, N/NE Af- rica, Cen- tral Asia	Various locations [@]								2.5-3.9

1330 * Müller et al. (2008)

1331 ‡ Petzold et al. (~~2008~~2009)

1332 # Linke et al. (2006)

1333 § Alfaro et al. (2004)

1334 ^μ Fialho et al. (2005)

1335 [°] Denjean et al. (2016); ^{%%} at 528 nm, ^{%%%} at 652 nm

1336 [&] Yang et al. (2009); ^{&&} at 375 nm, ^{&&&} at 470 nm, ^{&&&&} at 590 nm

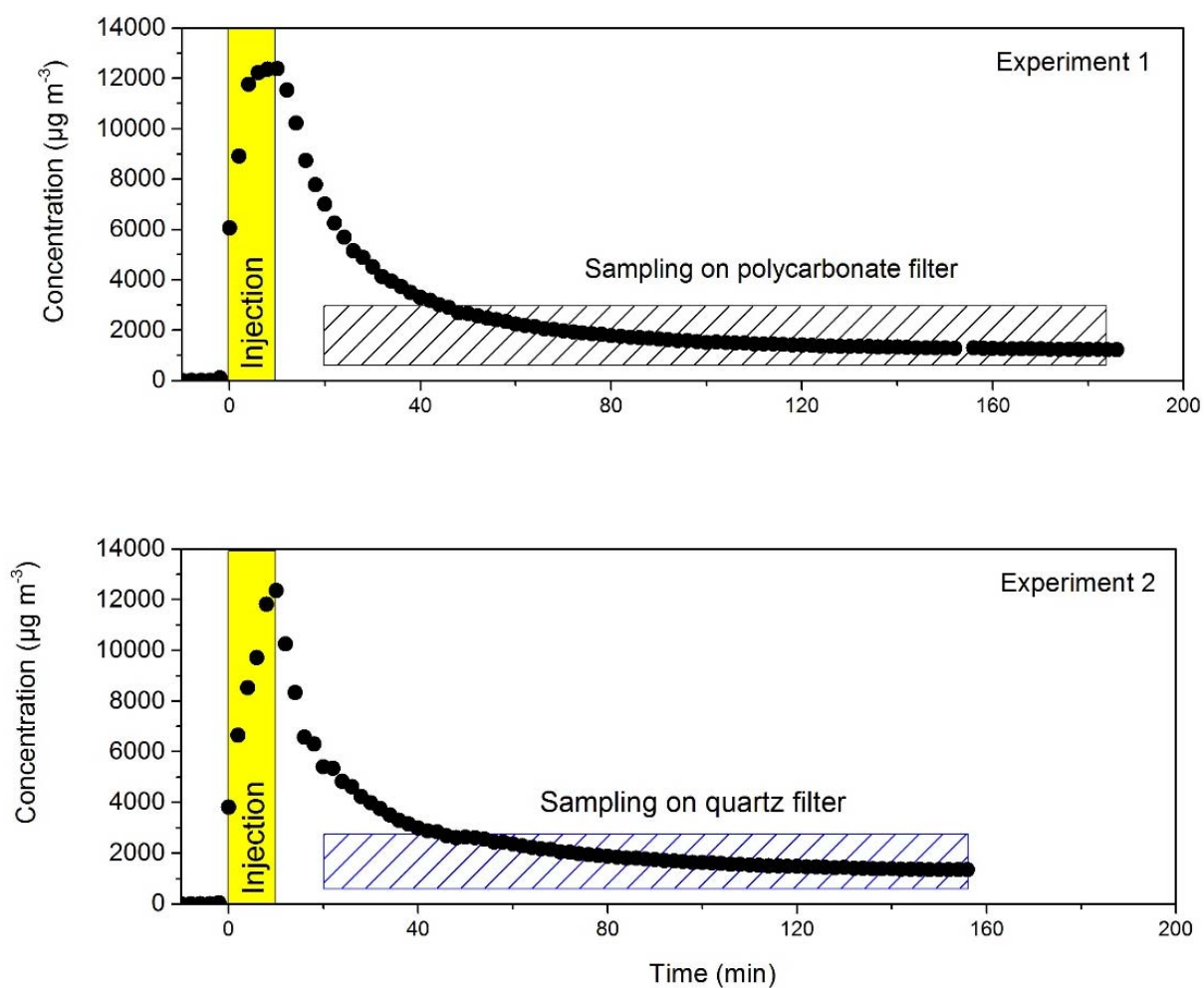
1337 [@] Mossmüller et al. (2012)

1338

1339

1340

1341 **Figure 1.** [Time series of aerosol mass concentration in the chamber for two companion experiments](#)
1342 [\(Libyan dust\).](#) ~~Time series of aerosol mass concentration in the chamber for the two companion experi-~~
1343 ~~ments (Libya sample).~~ Experiment 1 (top panel) was dedicated to the determination of the chemical
1344 composition (including iron oxides) by sampling on polycarbonate filters. Experiment 2 (bottom panel)
1345 was dedicated to the determination of the absorption optical properties by sampling on quartz filters.

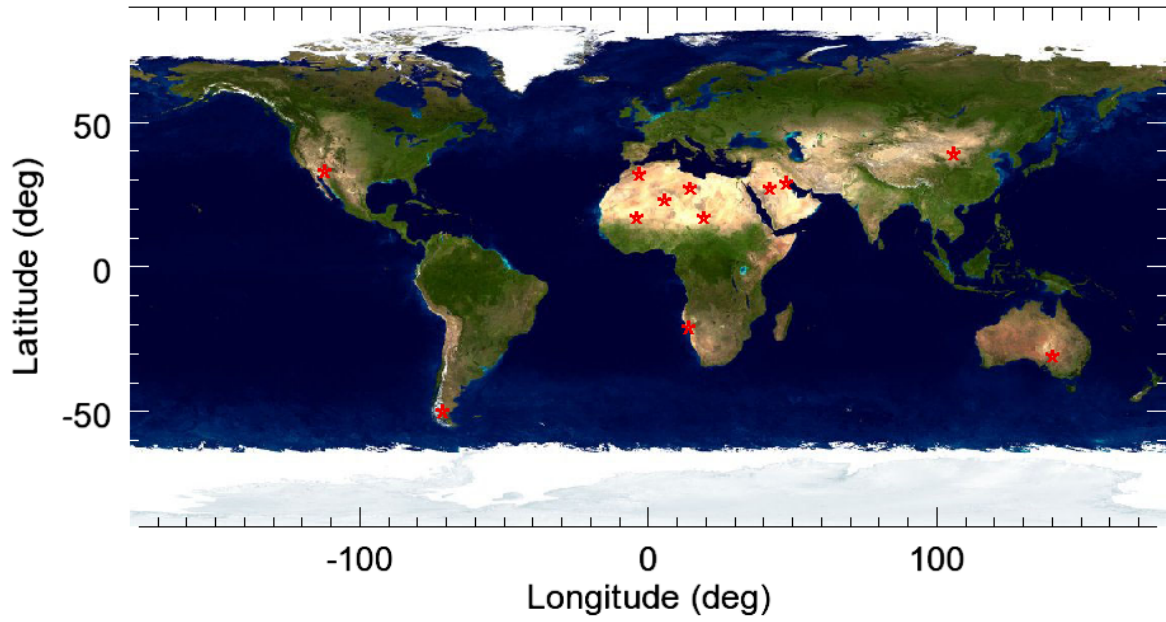


1346

1347

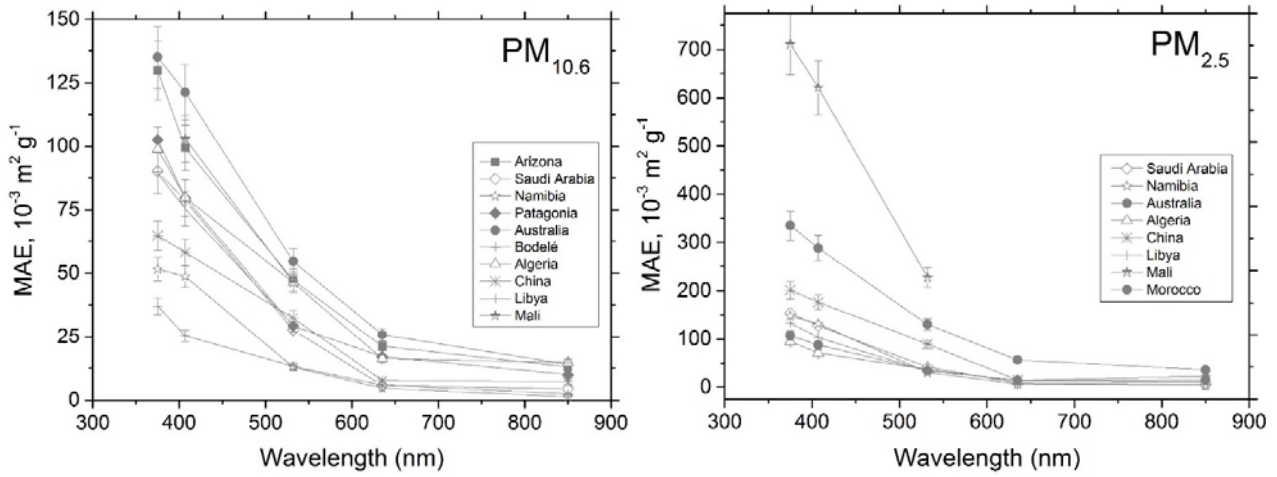
1348

1349 **Figure 2.** Locations (red stars) of the soil and sediment samples used to generate dust aerosols.



1350
1351

1352 **Figure 3.** Spectral dependence of the MAE values for the samples investigated in this study in the PM_{10.6}
1353 (left) and in the PM_{2.5} (right) mass fractions.



1354

1355 **Figure 4.** Illustration of the links between the MAE values and the dust chemical composition found in
1356 this study. Left column, from top to bottom: linear regression between the MAE values in the range from
1357 375 to 850 nm and the fraction of elemental iron relative to the total dust mass ($MR_{Fe\%}$) in the $PM_{10.6}$
1358 fraction; Middle column: same as left column but for the mass fraction of iron oxides relative to the total
1359 dust mass ($MR_{Fe\ ox\%}$) in the $PM_{10.6}$ size fraction; Right column: same as left column but in the $PM_{2.5}$ size
1360 fraction.

1361 ~~Illustration of the links between the MAE values and the dust chemical composition found in this study.~~
1362 ~~Left column, from top to bottom: MAE values between 375 and 850 nm versus the fraction of elemental~~
1363 ~~iron with respect to the total dust mass ($MR_{Fe\%}$) in the $PM_{10.6}$ fraction; Middle column: same as left~~
1364 ~~column but versus the mass fraction of iron oxides to the total dust mass ($MR_{Fe\ ox\%}$) in the $PM_{10.6}$ size~~
1365 ~~fraction; Right column: same as left column but in the $PM_{2.5}$ size fraction. The linear regression lines~~
1366 ~~between MAE and $MR_{Fe\%}$ and MAE and $MR_{Fe\ ox\%}$ are reported in each plot.~~

1367

1368

1369

1370

1371

1372

1373

1374

1375

1376

1377

1378

1379

1380

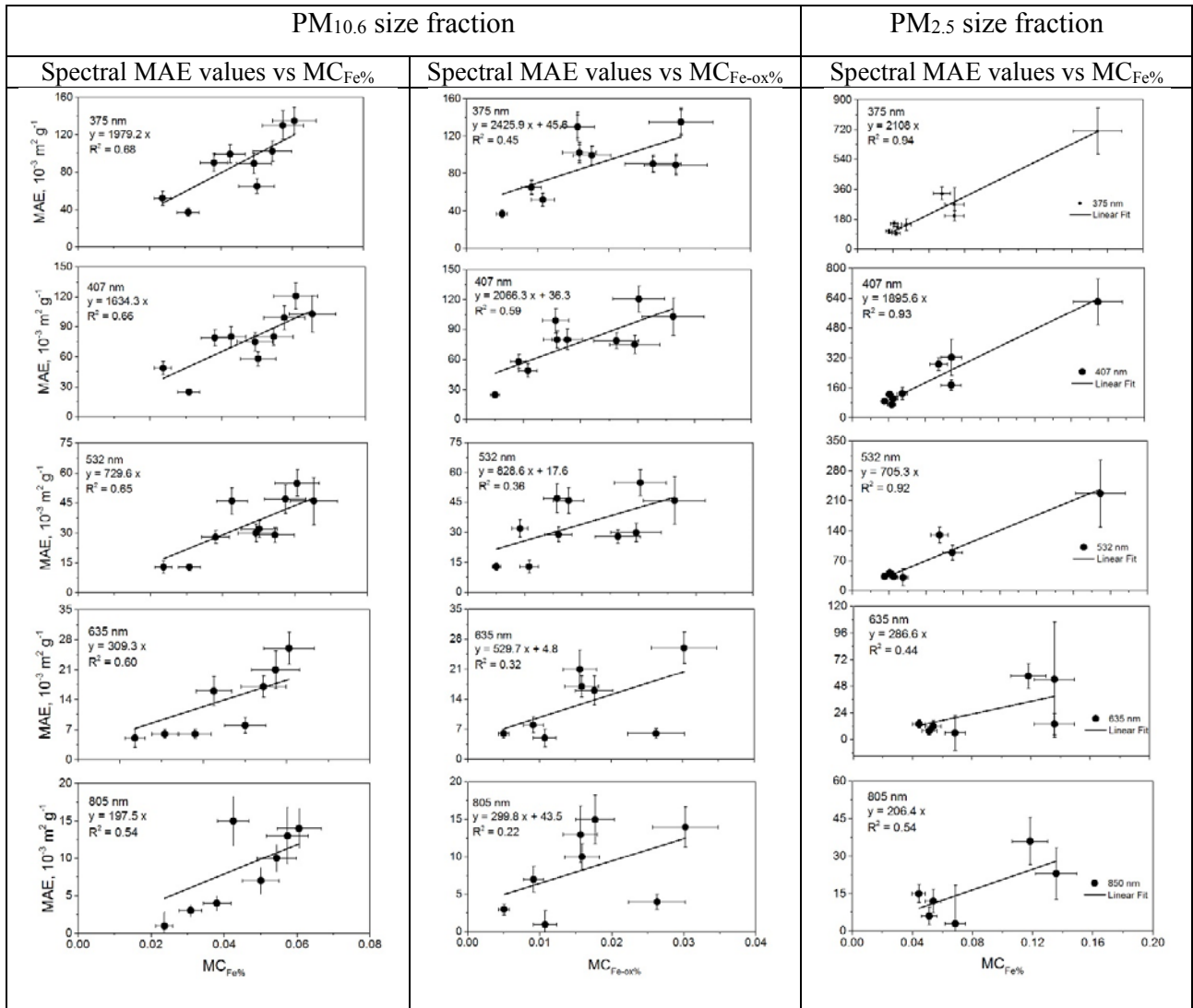
1381

1382

1383

1384

1385



1386
1387